Cell Reports
Physical Science

CellPress
OPEN ACCESS

Review

Photoresponsive Materials for Antibacterial Applications

Yawei Ren,[1,6] Hanpeng Liu,[1,6] Xiangmei Liu,[2,*] Yufeng Zheng,[3] Zhaoyang Li,[1] Changyi Li,[4] Kelvin Wai Kwok Yeung,[5] Shengli Zhu,[1] Yanqin Liang,[1] Zhenduo Cui,[1] and Shuilin Wu[1,7,*]

SUMMARY

Recently, photoactivated sterilization, as a rapid, effective, and antibiotic-free antibacterial method, has attracted increasing attention from researchers. Many outstanding photoresponsive materials, including photocatalysts, photosensitizers (PSs), and photothermal materials, have been developed and applied to microbial inactivation and to treat infectious bacterial diseases. This mini-review aims to provide insights gathered from studying photoresponsive antibacterial materials and systems, including (1) reactive oxygen species (ROS)-based photodynamic therapy (PDT) and (2) hyperthermia-based photothermal therapy (PTT). In addition, potential application fields for these methods, the remaining challenges to using photoresponsive materials for microbial inactivation, perspectives for the future, and prospective research directions are discussed in depth.

INTRODUCTION

Infectious bacterial diseases have always threatened the lives and health of human beings, especially in the eras before antibiotics and other effective therapeutic strategies. For instance, the infamous outbreak of the bubonic plague, also called the Black Death, which was caused by *Yersinia pestis* bacterial infections, claimed the lives of 30%–50% of the European population between 1347 and 1351.[1,2] Since the 1940s, many antibiotics have been developed and applied to fight pathogenic microorganisms.[3] However, the misuse or overuse of antibiotics has been inducing increasingly serious bacterial resistance, which stems from *de novo* mutations or from resistance genes that the bacteria acquire from other organisms. According to speculations from the World Health Organization (WHO),[4] by 2050, ~10 million people will die every year from diseases caused by bacterial resistance. No drugs are available to treat infectious diseases caused by superbugs.[5] Therefore, it is urgently necessary to develop effective therapeutic strategies that will inactivate bacteria without causing bacterial resistance.

Metal ion antibacterial agents and some natural bio-antimicrobial agents have already proven to be promising candidates. In recent years, research concerning microwaveocaloric therapy, sonodynamic treatment, and photoactivated therapy as effective and rapid antibacterial methods has attracted tremendous interest.[6,7] Photoactivated sterilization uses light irradiation at appropriate wavelengths, ranging from ultraviolet (UV) to near-infrared (NIR), to activate photoresponsive materials, which absorbs light energy to effectively kill pathogens in a short time by producing radical oxygen species (ROS) or/and hyperthermic conditions. This technique can avoid bacterial resistance by killing the bacteria rapidly, as compared to

[1]The Key Laboratory of Advanced Ceramics and Machining Technology by the Ministry of Education of China, School of Materials Science and Engineering, Tianjin University, Tianjin 300072, China

[2]Hubei Key Laboratory of Polymer Materials, Ministry of Education Key Laboratory for the Green Preparation and Application of Functional Materials, School of Materials Science and Engineering, Hubei University, Wuhan 430062, China

[3]State Key Laboratory for Turbulence and Complex System and Department of Materials Science and Engineering, College of Engineering, Peking University, Beijing 100871, China

[4]Stomatological Hospital, Tianjin Medical University, Tianjin 300070, China

[5]Department of Orthopaedics and Traumatology, Li Ka Shing Faculty of Medicine, The University of Hong Kong, Pokfulam, Hong Kong 999077, China

[6]These authors contributed equally

[7]Lead Contact

*Correspondence: liuxiangmei1978@163.com (X.L.), shuilinwu@tju.edu.cn (S.W.)

https://doi.org/10.1016/j.xcrp.2020.100245

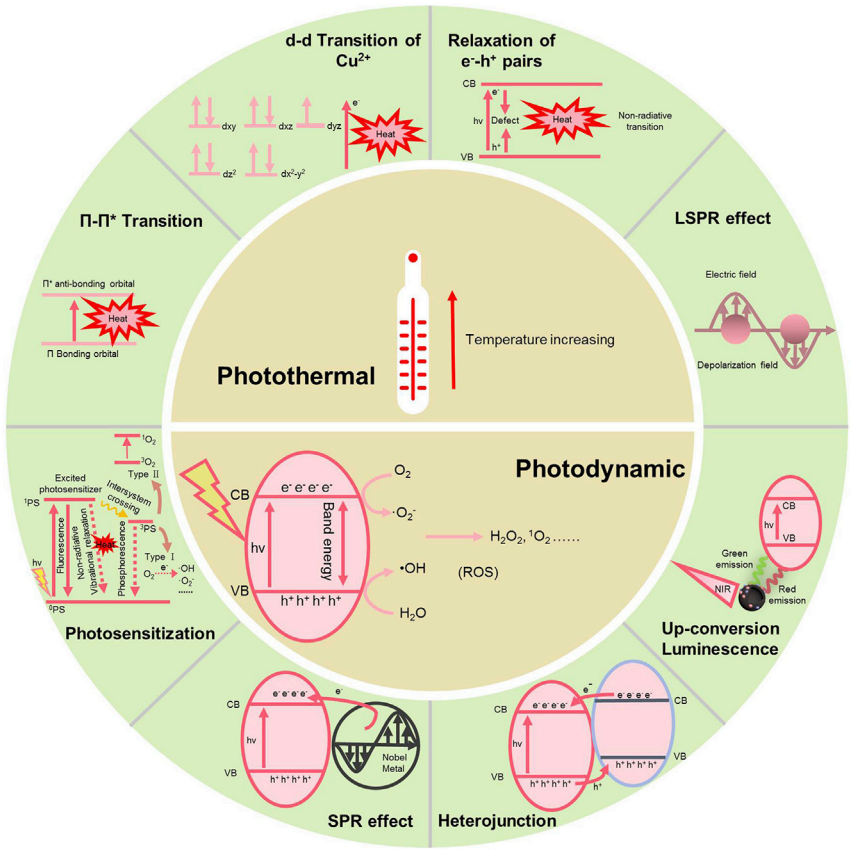

Figure 1. Outline of Photoresponsive Mechanisms
Outline of primary mechanisms of photothermal and photodynamic.

conventional antibiotic treatments. Another important advantage is that the newly developed treatment can target infected sites without damaging other organs or surrounding tissues because the position, strength, and time of the treatment can be conveniently controlled.[8]

This mini-review comprehensively considers recent representative studies concerning the development of photoresponsive systems for microbial inactivation. The antibacterial modes in these studies are categorized into two types: (1) ROS-based photodynamic therapy (PDT), and (2) hyperthermia-based photothermal therapy (PTT). The fabrication, characterization, and antibacterial activity of some typical photocatalysts, photosensitizers (PSs), photothermal materials, and heterostructures are also discussed, and the underlying mechanisms of photothermal and photodynamic effects are summarized in Figure 1. In addition, the potential applications of photoresponsive materials for microbial inactivation, as well as the remaining challenges to their use, are detailed in depth.

Photoresponsive Antimicrobial Materials Based on PDT

PDT involves combating pathogenic bacteria via ROS, which is a general term describing the chemical species formed by incomplete oxygen reduction. ROS mainly includes superoxide anion ($\cdot O_2^-$), hydrogen peroxide (H_2O_2), singlet oxygen ($^1O_2$), and hydroxyl radical ($\cdot OH$). It is widely accepted that ROS can bind to and damage bacterial membranes and cell walls, thereby destroying the bacterial

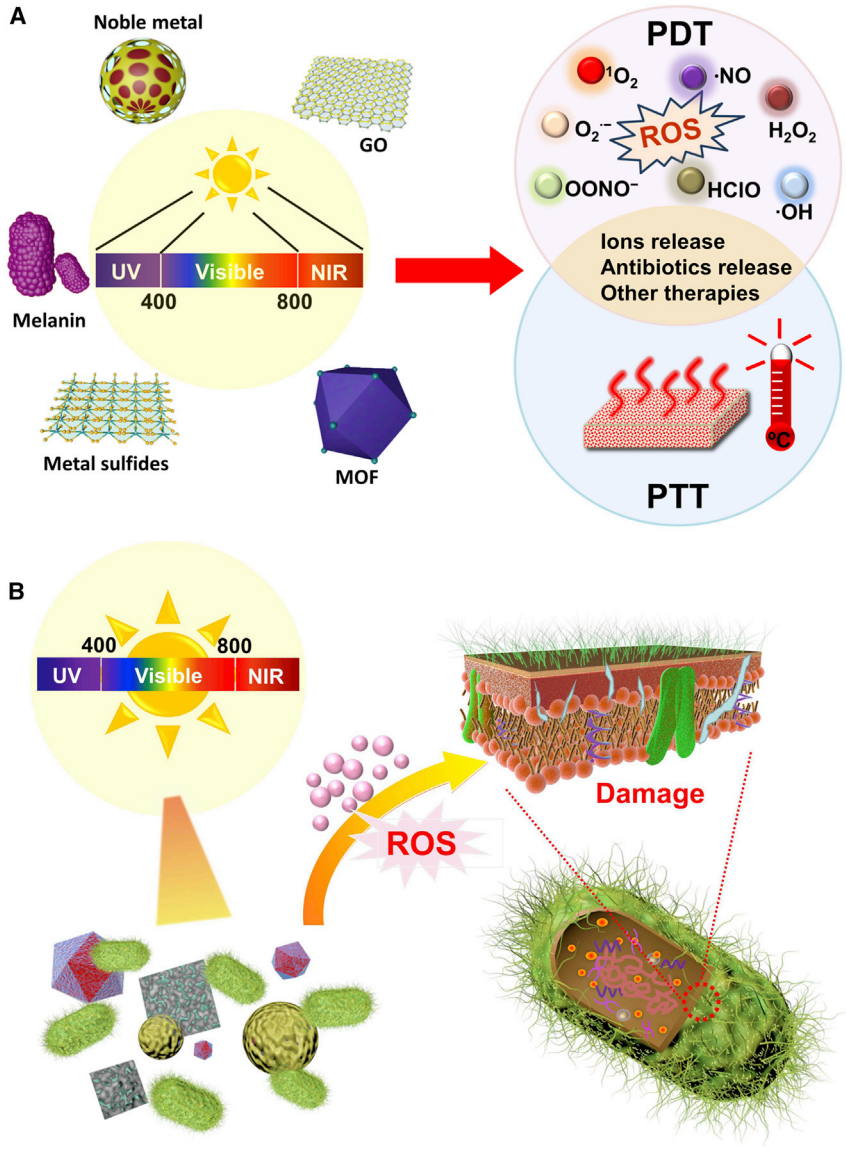

Figure 2. Illustration of Photoresponsive Antibacterial Systems

(A) Schematic illustration of photoresponsive antibacterial materials and systems.

(B) Schematic illustration of the specific mechanism of PDT.

defense system. ROS can also penetrate bacterial membranes, entering the cells to destroy proteins and lipids and, thus, directly or indirectly disrupting cellular respiration and other physiological activities (Figure 2).[6,9] With the increasing bacterial resistance to antibiotics, the PDT strategy is becoming one of the best substitutes for treating certain infectious bacterial diseases, and its popularity may be ascribed to the following attributes.[8] First, PDT is a broad-spectrum therapeutic mode because photoexcited ROS can act on the many metabolic pathways and cellular structures of various bacteria types, rather than on a single process or structure. Second, PDT is a rapid and highly effective treatment mode because it instantly produces and dissipates ROS and can very quickly combat bacteria once light has been irradiated. Most photocatalysts and PSs do not demonstrate antibacterial properties without light irradiation. Hence, bacteria cannot discern or develop

resistance against photocatalysts or PSs. Lastly, the serious damage PDT causes to bacteria makes it difficult for them to transmit their self-adaptivity to the next generation in a short time.[10]

It is worth mentioning, however, that PDT is less effective for Gram-negative (G^-) bacteria, such as *Escherichia coli* (*E. coli*), than for Gram-positive (G^+) bacteria, such as *Staphylococcus aureus* (*S. aureus*), due to their different membrane structures. Specifically, the outer membrane of G^+ bacteria is composed of multiple layers of loose, porous peptidoglycan (PG), which can be penetrated easily by small molecular compounds, polysaccharides, peptides, and other biomolecules. In contrast, the PG layer of G^- bacteria is relatively thin, but there is a dense lipopolysaccharide (LPS) and lipoprotein structure outside the cell wall that acts as a permeability barrier, making G^- bacteria less sensitive to ROS.[11] As illustrated in Figure 1, PDT can be achieved through various routes under light irradiation, including photocatalysts, PSs, surface plasmon resonance (SPR), and heterojunction and up-conversion luminescence, which are presented in the following sections.

Photocatalysts for Antibacterial PDT

Many traditional semiconductor materials are often used as photocatalysts, such as TiO_2,[12] ZnO,[13] and WO_3,[14] which have been studied both under *in vitro* and *in vivo* conditions to control and combat bacterial infection. Their antibacterial activity comes from ROS produced during the photoexcitation process.[9,15] To be specific, as shown in Figure 1, the electrons (e^-) excited on the conduction band (CB) reduce O_2 into $\bullet O_2^-$, while photoinduced holes (h^+) on the valence band (VB) oxidize H_2O to $\bullet OH$, which can be further converted to other types of ROS via various catalytic reactions.[16]

Due to the wide bandgap, however, most photocatalysts can only be driven by UV or shortwave visible light, which only makes up a small portion of solar light. To reduce their bandgaps and enhance their light absorption capabilities, many strategies have been implemented such as elemental doping,[17,18] changing their size and structure,[19] and combining them with other semiconductors.[20]

Dating back to 2009, graphic carbon nitride (g-C_3N_4) is a metal-free photocatalyst,[21] and in 2014, Huang et al.[22] proved that g-C_3N_4 exhibited antibacterial effects against *E. coli* under visible light irradiation. Although g-C_3N_4 possesses a narrower band gap and a better adsorption capacity than traditional photocatalytic antibacterial agents, it still, like most photocatalysts, faces the problem of rapid electron-hole recombination. In a recent work,[23] Zn atoms were doped into the clearance of the g-C_3N_4 structure to optimize its photocatalytic performance. Thanks to the increased vacancy resulting from the generated lattice defects, the absorption property of g-C_3N_4 increased, and the absorption edge appeared as an evident redshift.

Apart from g-C_3N_4, many other metal-free photocatalysts have attracted widespread attention. The size and structure of red phosphorus (RP) and black phosphorus (BP) endow them with unique physicochemical, optical, and biological properties, which make them promising photoresponsive materials for using PDT against bacterial infections.[24] For example, the present authors' research group deposited RP films via chemical vapor deposition (CVD) on the surface of a Ti substrate, which can be used as a surgical implant.[25] The results demonstrated that the Ti-RP combination exhibited a broad-spectrum light response, with sharply promoted light absorption in the NIR region, which makes up ~44% of the solar spectrum. The strong signal of detected $\bullet O_2^-$ and $^1O_2$ under 808 nm irradiation verified

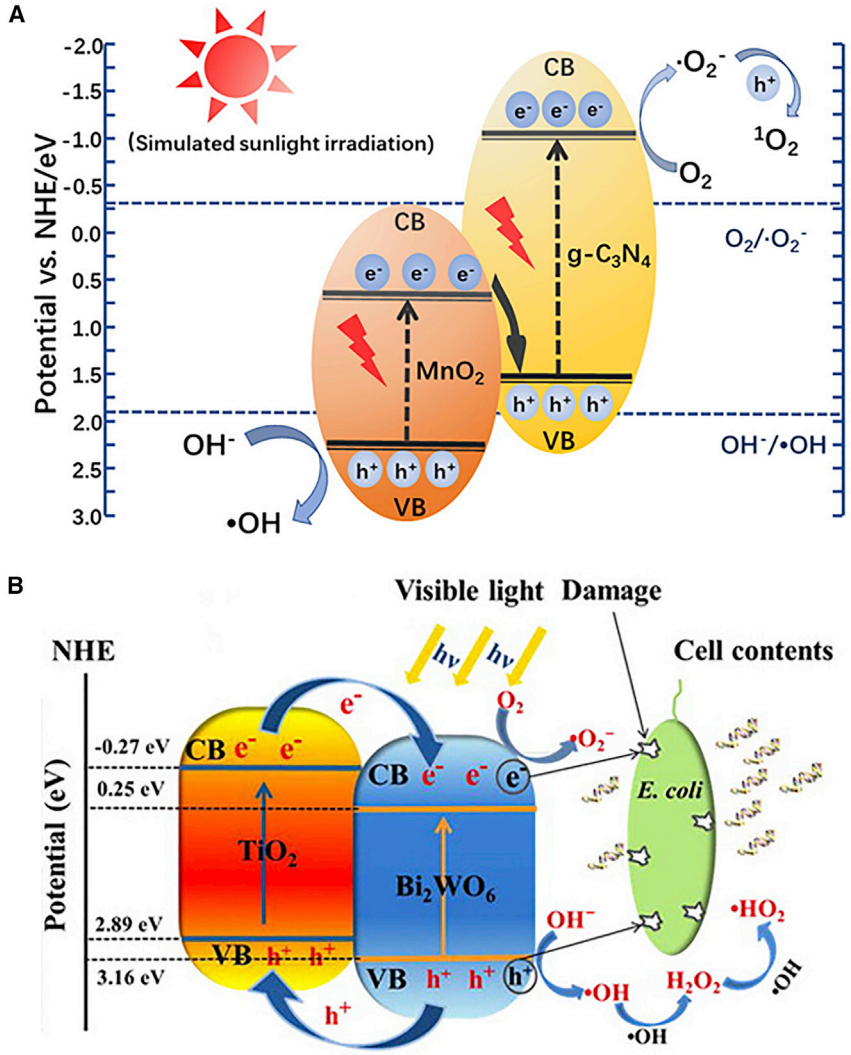

Figure 3. Heterojunctions for Enhanced Photocatalytic Disinfection

(A) Schematic illustration of enhanced photocatalytic properties of MnO_2/g-C_3N_4 heterostructure. Reproduced with permission from Wu et al.[27] Copyright 2019, Elsevier BV.

(B) Schematic illustration of TiO_2–Bi_2WO_6 binanosheets for enhanced photocatalytic disinfection of *E. coli*. Reproduced with permission from Jia et al.[29] Copyright 2016, American Chemical Society.

that RP was an ideal NIR-activated antimicrobial agent for effectively eradicating bacterial infections on the surface of implants.

Heterostructures as Photocatalysts

In addition to narrow band gaps, a factor that reduces the photocatalytic property is the rapid recombination of photogenerated electron-hole pairs in single semiconductors.[26] A effective approach to this problem is constructing heterojunctions with two or more semiconductors, which can promote charge separations and transfers. For example, an MnO_2/g-C_3N_4 heterostructure coating was developed on the surface of a Ti implant by the present authors' research group.[27] As shown in Figure 3, in this system, MnO_2 and g-C_3N_4 formed a Z-scheme heterojunction, leading to the rapid migration of e^- from the CB of MnO_2 to the VB of g-C_3N_4. The rapid charge transfer significantly promoted the ROS yield, which denatured the proteins

and damaged the DNA in the bacterial cells. *In vitro* antibacterial tests confirmed that the coating achieved a superior antibacterial efficacy of 99.26% and 99.96% against *E. coli* and *S. aureus*, respectively, after being exposed to visible light for 20 min.

Compared with one-dimensional (1D) materials, 2D nanosheets have a higher specific surface area, more active sites for photocatalytic reactions, and shorter perpendicular distances for electron and hole mobilization, endowing them with better photocatalytic properties.[28] Jia et al.[29] prepared a TiO_2-Bi_2WO_6 nanosheet to deal with *E. coli* (Figure 3). After being composited with Bi_2WO_6, the adsorption toward the visible light of TiO_2 and the separation of h^+-e^- pairs were obviously promoted. The result disclosed that bacterial membranes were ruptured, and the substance inside the bacterial cells, such as 16S rDNA and total protein, flowed out, demonstrating that their prepared heterostructure effectively killed bacteria via enhanced PDT under visible light.

PSs for Antibacterial PDT

Similarly, some organic PSs can also generate ROS in the presence of light and oxygen to kill nearby pathogenic microorganisms. However, there are some intrinsic differences between PSs and photocatalysts. PSs are mainly small, organic molecules, while photocatalysts are typically semiconductive, inorganic materials. In addition, the ROS generation mechanism is quite different between the two. As shown in Figure 1, after light irradiation, a PS accepts the energy of photons and is excited from the ground state to the singlet state (^{1}PS). The unstable ^{1}PS quickly releases electrons or energy to reach the longer-lived triplet state (^{3}PS), while generating ROS to destroy pathogens.[10] There are two predominant mechanisms for the photochemical reactions. The type I reaction is based on electron transfer. To be specific, ^{3}PS reacts with biomolecules, such as lipids, proteins, and nucleic acids, generating free radicals and radical ions, which subsequently react with O_2 or H_2O, leading to the generation of ROS. The type II reaction is based on energy transfer from ^{3}PS to O_2, which directly forms $^1O_2$. After the reactions are complete, PS molecules return to their ground states and participate in the next cycle of reactions.[30,31]

Porphyrins,[32] phthalocyanines,[33] phenothiazines,[34] and many other organic PSs have been widely used in PDT, and they have exhibited strong antibacterial activity. For example, a cationic porphyrin derivative was proved to be effective for the photodynamic inactivation of *S. aureus*, *Pseudomonas aeruginosa*, and *Candida albicans* biofilms.[35] However, when a PS is used alone, the efficiency of PDT is restricted by the poor solubility of PS and the limited intracellular O_2 content.[36] A convenient strategy for increasing the therapeutic effect is to load PSs with photocatalysts.[37,38] When combined with photocatalysts, the ROS yields can be significantly enhanced, beyond what PSs or photocatalysts can achieve alone. For instance, Sułek et al.[39] used impregnation methods to prepare halogenated porphyrin (F_2POH) and its zinc derivative (ZnF_2POH) on the surface of TiO_2. This TiO_2-based hybrid material showed a higher yield of $^1O_2$ and a stronger photoresponsive antibacterial ability than pure TiO_2 or porphyrin alone because of the synergistic effect of porphyrins and TiO_2. In another work, Senthilkumar et al.[40] encapsulated meso-tetra (4-sulfonatophenyl) porphyrin (TSPP) with ZnO, which endowed the hybrids with much stronger photocatalytic activity than either pristine ZnO or porphyrin. Hence, again, the hybrid showed superior PDT efficacy against bacteria.

SPR Effect for Enhanced Optical Absorption

Some noble metals (Au and Ag) and metallic compounds (CuS) can be excited to produce SPR, aiming to enhance the effect of PDT. Possible mechanisms for

enhancing the SPR effect of photocatalysis under visible light have been discussed previously.[41] The first option is the charge transfer mechanism in which the plasmon resonance activates electrons in the noble metals, which can then transfer to the CBs of the photocatalysts.[42] Another possible mechanism holds that the irradiation near the plasmon resonance frequency of noble metals can result in intense local electric field enhancement on the surfaces of photocatalysts, accelerating the separation of e^{-}-h^{+} pairs.[43] For example, Ag/AgBr-loaded mesoporous silica nanomaterials (Ag/AgBr/MSNs) were synthesized by the authors' research group.[44] The results showed that the visible light absorption of the hybrid was much higher than that of Ag or AgBr alone. In addition, the photocatalytic activity was significantly enhanced with more ROS production. After 15 min of simulated sunlight irradiation, the Ag/AgBr-loaded system exhibited a highly effective antibacterial rate of 99.99% against *E. coli*, which was ascribed to the SPR effect of the Ag nanoparticles (NPs).

In addition to semiconductors, the light absorption and photocatalytic properties of PSs can be strengthened by the SPR effect of noble metals combined with PSs via loading or immobilizing processes. For example, Elashnikov et al.[45] grafted modified porphyrin onto the surface of Ag NPs. The hybrids exhibited more outstanding antibacterial activity than pure porphyrin or Ag NPs alone under light-emitting diode (LED) illumination at 405 nm, which corresponded to the absorption peak of porphyrin and the SPR region of Ag NPs.

The light-harvesting capacities of semiconductors and PSs can also be enhanced by metals other than Ag, such as Au and Bi. For example, Li et al.[46] used Au nanorods to decorate Bi_2WO_6 nanosheets (Au@Bi_2WO_6). Their results disclosed that the light absorption and photocatalytic properties of pure Bi_2WO_6 were significantly enhanced, resulting in rapid photocatalytic microbial inactivation against both *E. coli* and *S. aureus* (Figure 4), which was ascribed to the SPR effect of the Au nanorods.

Up-Conversion Luminescence Materials

The challenge of using UV-visible (vis) light as a light source for PDT is that it has a poor penetration ability compared to NIR light. Unfortunately, however, most semiconductors cannot respond to NIR light. To overcome this restriction, up-conversion nanoparticles (UCNPs) have been developed and are attracting increasing attention because of their unique performance at converting the excitation of long-wavelength light into short-wavelength light, which can more easily trigger the photodynamic actions of visible light-responsive photocatalysts. Hence, in some cases, photoresponsive systems consisting of up-conversion materials and semiconductors or PSs have been developed for use with the PDT strategy. For instance, in recent work by the current authors' research team, a traditional semiconductor (TiO_2) was doped with proper content Er, which is one of the most frequently used rare earth elements in up-conversion materials.[47] The luminescence spectra of the doped TiO_2 proved that it could transform the NIR (808 nm) into the visible region, which is more easily harvested to produce ROS to rapidly kill bacteria. In another work, Yin et al.[48] prepared $NaYF_4$:Er/Yb/Mn UCNPs, modified by methylene blue (MB), and loaded the UCNP/MB into polymeric hydrogel. To realize a deeper penetration, a 980-nm laser was used as a light source. Under 980 nm NIR light irradiation, the emission peak of the UCNPs was located at 650 nm, which was well matched with the strong absorption region of MB. In other words, the emission UCNPs converted the incident light of 980 nm into 650 nm red light, which was then used to excite the MB and produce ROS. Therefore, the UCNP/MB-doped hydrogel showed excellent antimicrobial efficiency, assisted by the electrostatic interaction of cations with the bacterial membrane.

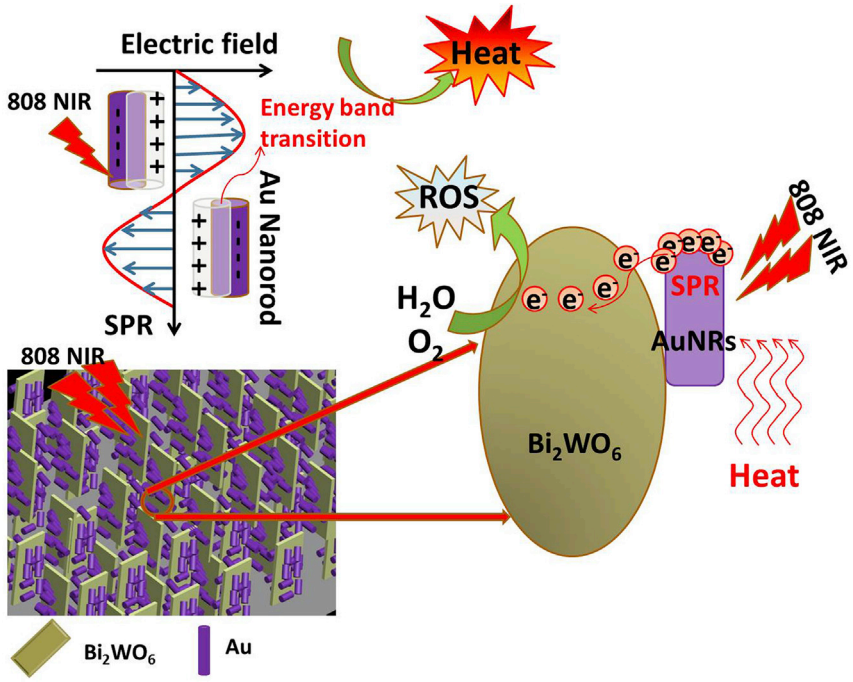

Figure 4. SPR for Enhanced Bacteria-Killing Effects

Schematic illustration of enhanced photocatalytic activity of the Au@Bi_2WO_6 composites for rapid bacteria killing under NIR through SPR effects. Reproduced with permission from Li et al.[46] Copyright 2019, Elsevier BV.

Synergistic Antibacterial System Based on PDT

Despite ROS having strong bactericidal activity by participating in certain bacterial chemical reactions, these species have a short lifetime and short penetration distance; that is to say, only those ROS generated on the surface of or near infected sites can effectively kill bacteria, which hinders the application of PDT strategies. To overcome this problem, many disinfection systems have been designed to combine PDT with other sterilization methods, thus realizing a higher antibacterial efficacy.[49,50]

It is widely accepted that Ag-based nanomaterials have a broad-spectrum bactericidal effect because the slow release of Ag^+ can inflict physical damage to cell membranes and the inside substances of bacterial cells.[51] However, these nanomaterials are also considered inherently toxic when used excessively. Therefore, in recent years, many antibacterial systems have been constructed to combine Ag^+ with PDT to combat bacteria. For example, a hybrid Ag_3PO_4/graphene oxide (GO) coating was established based on the electrostatic adsorption between Ag_3PO4 and GO to attain rapid sterilization (Figure 5).[52] Under the irradiation of a 660-nm light for 15 min, the coating's antimicrobial efficacy against *E. coli* and *S. aureus* was 99.53% and 99.66%, respectively. The released Ag^+ endowed the surface with physical bacteria-killing performance. By inhibiting the recombination of e^--h^+ pairs and enhancing the light absorption of GO, the system, with a tunable band gap, achieved, through the synergistic action of PDT and released Ag^+, much better antibacterial efficacy than a single component could have achieved alone. The generated ROS enhanced the permeability of the bacterial membrane, accelerating the rate at which Ag^+ entered the cells. In addition, the dosage of released Ag^+ was controlled by the GO nanosheets, which had a large specific

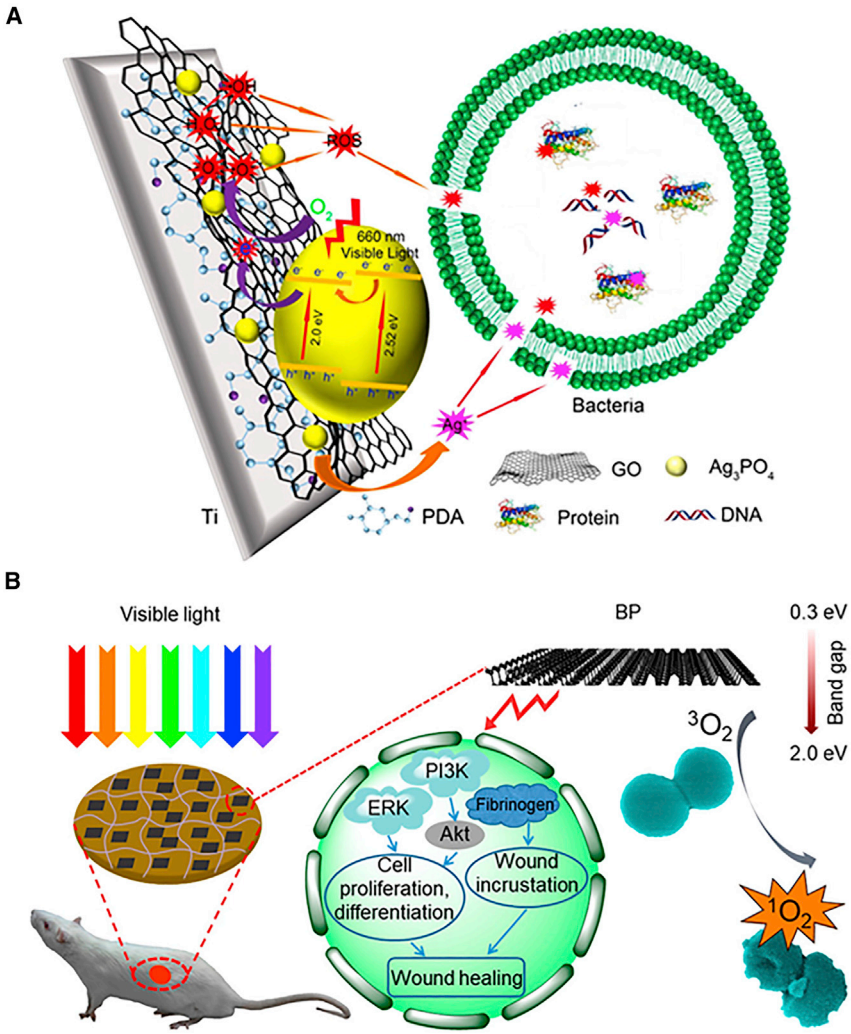

Figure 5. Synergistic Antibacterial Platform Based on PDT

(A) Schematic illustration of hybrid Ag_3PO_4/GO coating with synergistic antibacterial behavior of Ag^+ and ROS to damage the bacterial cell membranes, proteins, and DNA. Reproduced with permission from Xie et al.[52] Copyright 2018, American Chemical Society.

(B) Schematic illustration of BP-loaded CS hydrogel for sterilization and acceleration of wound healing under visible light. Reproduced with permission from Mao et al.[55] Copyright 2018, American Chemical Society.

surface area that not only reduced the cytotoxicity of the silver ions for normal tissues but also sustained stable antibacterial properties over a longer period.

Chitosan (CS), as a natural antimicrobial, is claimed to effectively kill many kinds of pathogens and fungi through electrostatic action.[53] Besides its intrinsic disinfection ability, CS exhibits terrific biodegradability and biocompatibility, which makes it a good carrier material.[54] Therefore, much effort has been made to develop a CS and PDT synergistic antibacterial system. For example, a BP-loaded CS hydrogel was constructed via electrostatic interaction (Figure 5).[55] In the presence of simulated solar light, within 15 min, the hybrid hydrogel evidenced an antibacterial rate of 98.90% and 99.51% against *E. coli* and *S. aureus*, respectively, due to the synergy between CS and PDT. In addition, the degradable BP products were confirmed to induce signaling pathways, stimulating the proliferation and differentiation of

fibroblasts by upregulating fibrinogen expression, thus hastening wound healing. In addition to the information outlined above, synergistic sterilization systems composed of PDT and other antimicrobial agents, such as quaternary ammonium compounds (QACs),[56] cyclodextrin (CD),[57] and carbon dots,[58] have been extensively studied, and many advances have already been made.

Photoresponsive Antimicrobial Materials Based on PTT

Under light stimulation, many kinds of materials, including noble metal nanomaterials,[59,60] metallic oxides,[61,62] metallic sulfides,[63,64] carbon-based materials,[65] phosphorus,[9,66] and polymeric nanocomposites,[67,68] can convert solar energy into heat, which can also kill pathogenic bacteria. This therapeutic strategy is called PTT, and the materials used are called photothermal agents (PTAs). As previously mentioned, NIR light (700–1,300 nm) more efficiently penetrates skin and tissue, with minimal damage to healthy sites, compared to UV and visible light; thus, it is suitable for biological applications, especially for deep disinfection[6,69] and targeted antitumor treatments.[66,70,71] Because local hyperthermia damages the bacterial structure, disrupts cell membrane permeability, and ultimately results in bacterial death, PTT has a broad-spectrum antibacterial efficiency and will not lead to bacterial resistance or side effects.[72] Notably, according to the different features of the materials used, Xu et al.[73] divided the photothermal mechanism into three categories: (1) the localized SPR (LSPR) effect, (2) electron-hole generation and relaxation, and (3) the conjugation or hyperconjugation effect.

Noble Metals for Antibacterial PTT

As mentioned above, noble metal NPs have been widely used to inactivate microorganisms, and they are promising PTAs due to their LSPR effect. When absorbing light energy, they can transfer it into heat via the surface plasmons nonradiative decay process. The light absorption ability of noble metals is relevant to their sizes, shapes, distributions, and surface chemical states. When their sizes and shapes are appropriately altered, they can show significant LSPR properties, which can endow them with photothermal properties under NIR irradiation; thus, they kill bacteria via PTT.[59,74] For instance, Zhao et al.[59] synthesized triangle silver nanoplates (Tri-Ag), whose absorption was tuned to the NIR region by a simple, one-step, seedless synthetic method. Their results showed that the photothermal conversion efficiency of Tri-Ag was up to 58.67% under 808 nm laser irradiation, which endowed the material with good photothermal performance. This Tri-Ag exhibited a high bactericidal efficacy of >90% against both *E. coli* and *S. aureus*. Even for two typical drug-resistant bacteria, extended spectrum β-lactamase (ESBL) *E. coli* and methicillin-resistant *S. aureus* (MRSA), the corresponding antibacterial efficiency of the material reached up to 90.1% and 87.0%, respectively, more than that of spherical Ag NPs. In another work, bimetallic Au-Ag NPs were successfully manufactured through the seed-mediated growth method, using *E. coli* as the reducing agent; these NPs exhibited a more remarkable PTT effect than Au or Ag NPs alone (Figure 6).[60] It is worth mentioning that in addition to photothermal sterilization, Au-Ag NPs have other clinical applications; they could, for example, achieve the ultrafast colorimetric detection of H_2O_2 without 3,3′,5,5′-tetramethylbenzidine and peroxidase, an outcome that could even be observed by visual inspection.

Metal-Organic Framework-based Materials for PTT

Recently, metal-organic frameworks (MOFs), porous, crystalline materials made up of organic and metal units held together by coordination bonds, have been attracting great attention because of their flexible morphology, structure, size, and tunable compositions.[75,76] By changing the organic ligands or metallic nodes, MOFs can be

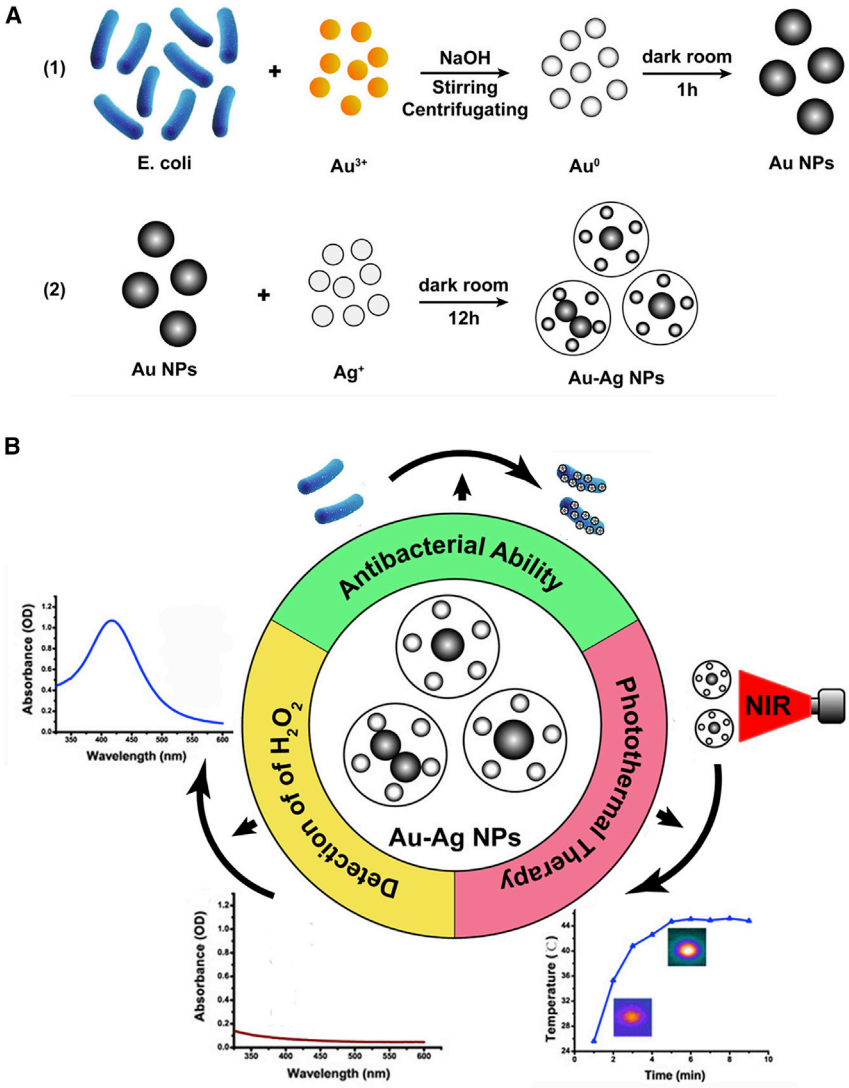

Figure 6. Bimetallic Au-Ag NPs for PTT

(A) Schematic illustration of the preparation process of bimetallic Au-Ag NPs with core-shell structure through seed-mediated growth method. Reproduced with permission from Jiang et al.[60] Copyright 2020, American Chemical Society.

(B) Schematic illustration of the applications of bimetallic Au-Ag NPs in the biomedical field. Reproduced with permission from Jiang et al.[60] Copyright 2020, American Chemical Society.

endowed with various specific properties for different applications. For example, as a kind of MOF, Prussian blue (PB) nanotubes have demonstrated photothermal performance under NIR light.[77] Although the specific mechanism of these materials is not fully understood, they have been widely used as PTAs for treating tumors and bacterial infections.[78,79] They have also been approved for use in clinical treatment by the US Food and Drug Administration due to their excellent biocompatibility and biosafety. However, during light irradiation, a single MOF has some drawbacks, such as low photothermal conversion efficiency. Therefore, researchers have developed some methods to strengthen the photothermal performance or assist in the PTT effect of MOFs. For example, recently, the present authors' research group used density functional theory (DFT) calculations to guide the doping of Zn into PB MOF (ZnPB) with different doping levels; thus, the photothermal performance and

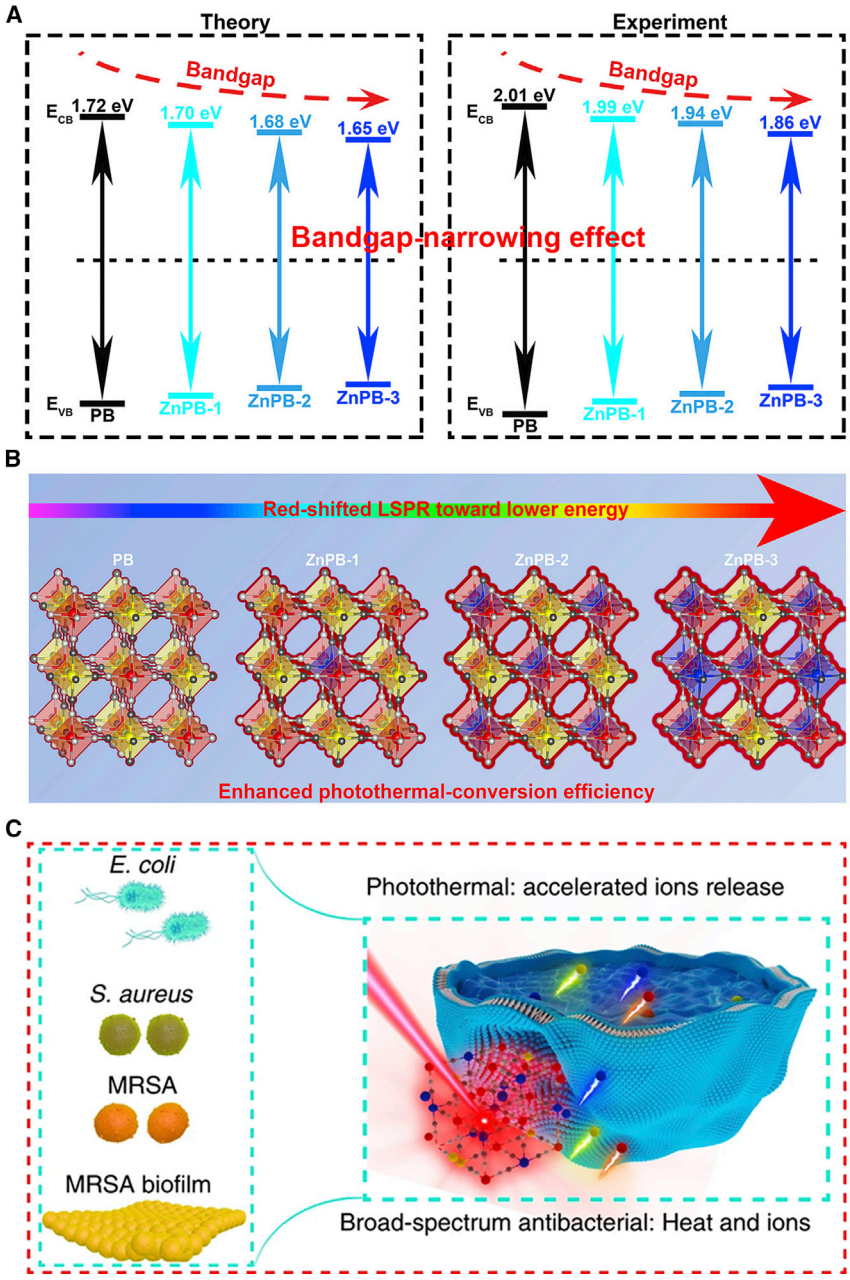

Figure 7. ZnPB for Synergistic Bacteria Killing

(A) Schematic illustration of narrowed band gap of ZnPB with different Zn doping density. Reproduced with permission from Li et al.[80] Copyright 2019, Springer Nature.

(B) Schematic illustration of enhanced photothermal conversion efficiency of ZnPB. Reproduced with permission from Li et al.[80] Copyright 2019, Springer Nature.

(C) Schematic illustration of mechanism of synergistic bacteria killing of ZnPB. Reproduced with permission from Li et al.[80] Copyright 2019, Springer Nature.

released ions of ZnPB were optimized (Figure 7).[80] The results disclosed that the band gap narrowing effect occurred with red-shifted LSPR toward the lower energy region as the Zn doping density was increased, which significantly enhanced the NIR absorption of ZnPB. This kind of PB showed broad-spectrum antibacterial effects against both G^+ and G^- *in vitro* and *in vivo*. It also obviously eradicated the MRSA

biofilm, which was formed by the self-produced extracellular polymeric substances of the bacteria and could encapsulate the bacteria as a protective barrier. This highly effective antibacterial activity of ZnPB was ascribed to the synergistic action of PTT and the released Zn^{2+}. The released Zn^{2+} also promoted wound healing by upregulating the expression of genes involved in tissue remodeling. In another work,[81] the authors' research team prepared nanocomposites of humic acid (HuA) and zeolitic imidazole framework-8 (ZIF-8) through the *in situ* growth of ZIF-8 on the surface of modified HuA (Figure 8). Within 20 min, this exhibited a highly effective bactericidal rate of 99.59% and 99.37% against *S. aureus* and *E. coli*, respectively, because of the synergy of PTT and the released Zn^{2+}.

In addition to Zn doping, electrostatic adsorption was used to assist in the PTT effect of a hydrogel composed of quaternary ammonium and double-bond modified CS and PB MOF particles (Figure 8), thus effectively killing bacteria.[82] In this system, the surrounding bacteria were tightly captured by the hydrogel through electrostatic absorption; then, the normal bacterial metabolism and respiration were suppressed by perturbing the surface potential of the bacterial membrane. Hence, the PTT killed these bacteria rapidly with an efficacy of 99.97% and 99.93% against *S. aureus* and *E. coli*, respectively.

Metal Sulfides for PTT

Over the last few decades, various metal sulfides have been applied in the biomedical fields due to their distinctive structures and properties.[64,83] Studies have disclosed that these sulfides possess a powerful NIR absorption ability, which makes them highly efficient and promising PTAs. As a representative of these metal sulfides, CuS is a p-type semiconductor following a large number of hole carriers and based on intrinsic Cu deficiencies in their lattice, which can cause the LSPR phenomenon to take the form of a different mechanism from that of noble metals. In addition, the d-d energy band transition of Cu^{2+} can significantly enhance PTT performance via NIR irradiation.[84] For example, in a 808-nm laser-driven system, CuS NPs exhibited strong photothermal sterilization performance due to the d-d energy band transition of Cu^{2+} (Figure 9).[64] Cu^{2+} was also found to promote wound healing due to its stimulation of cell proliferation. Therefore, the synthesized CuS NPs were considered excellent wound dressings, which could both release antibacterial effects and promote skin tissue regeneration.

Various transition-metal dichalcogenides, such as MoS_2, WS_2, and TiS_2, have also displayed high photothermal conversion efficiencies under NIR irradiation. Taking MoS_2 for example, its band gap can vary from 1.8 to 1.2 eV, depending on its thickness. By tuning the thickness and morphology of MoS_2, its spectral response edge can be adjusted to NIR, which makes it an ideal PTA for antibacterial platforms and antitumor treatments.[63,85] Similarly, Zhang et al.[86] discovered that CuS@MoS_2 hydrogel had a higher photothermal conversion efficiency than CuS hydrogel. MoS_2 could markedly enhance the hyperthermia phenomenon and ROS production, ultimately leading to bacterial death. Under the irradiation of 660 nm + 808 nm light, 99.3% of *E. coli* and 99.5% of *S. aureus* were killed within 15 min.

Non-metallic PTAs

Although metal elements play crucial roles as trace elements in the physiological activity of the body, their long degradation periods and probable residues may cause severe side effects. In view of this, non-metallic PTAs have attracted considerable attention. Among them, carbon and various carbon-based materials have been considered the most promising photoresponsive biological materials due to their

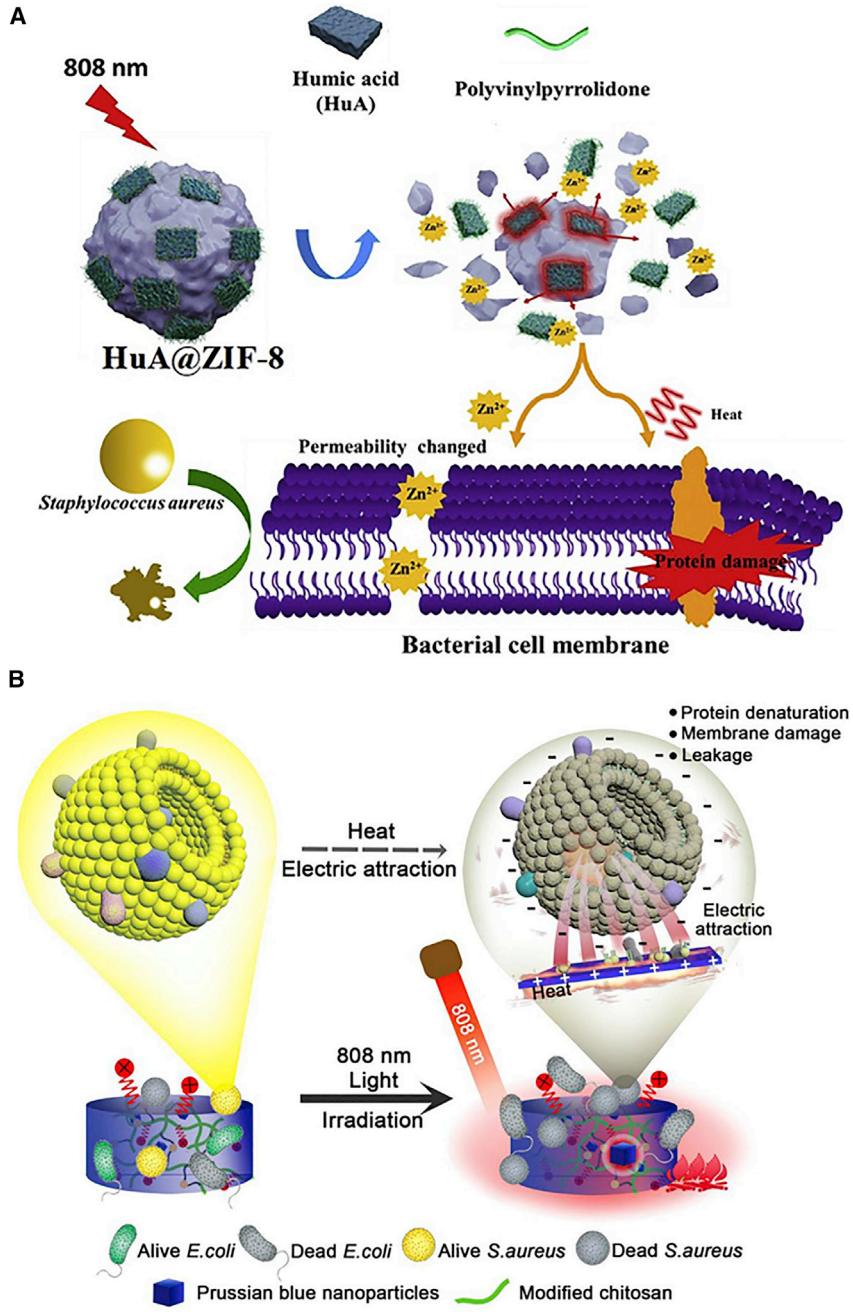

Figure 8. MOF-Based Composite Materials for PTT

(A) Schematic illustration of HuA@ZIF-8 for rapid bacteria killing by Zn^{2+}-assisted PTT. Reproduced with permission from Liu et al.[81] Copyright 2020, Elsevier BV.

(B) Schematic illustration of PB-strengthened CS hydrogels for rapid wounds through PTT and electrostatic absorption. Reproduced with permission from Han et al.[82] Copyright 2020, Elsevier BV.

strong optical absorptions, superior stabilities, high quantum efficiencies, and biosafety. The underlying photothermal mechanism of these materials is that photo-excited electrons can return to the ground state by emitting fluorescence or nonradiative relaxation, producing heat during this course of action.[65,87] Kim et al.[88] first reported carbon nanotubes (CNTs) as exhibiting photothermal antibacterial

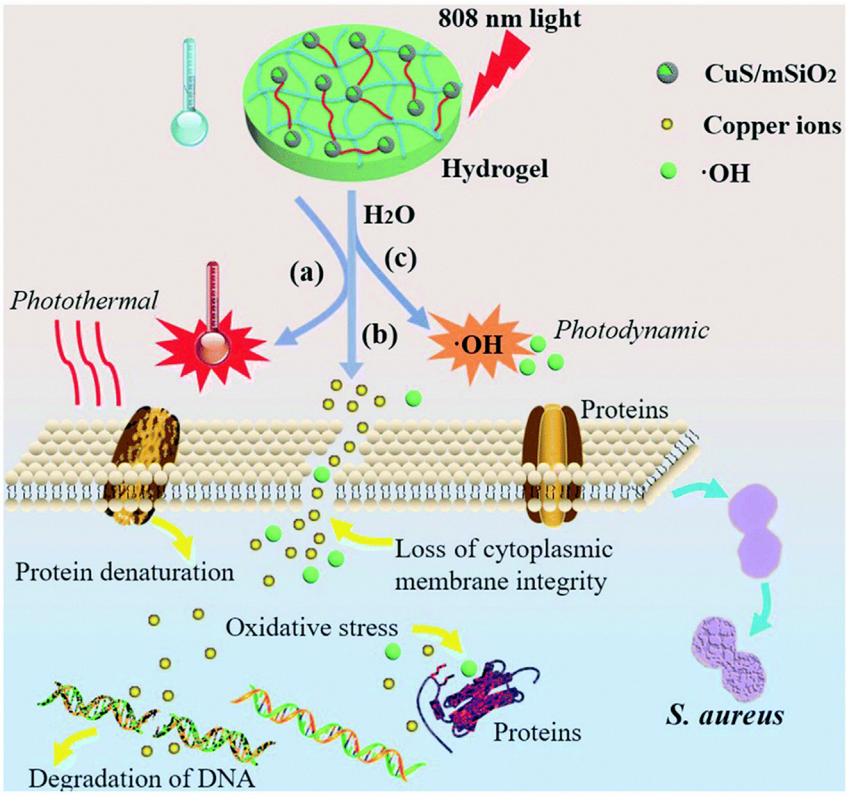

Figure 9. CuS-Containing Hybrid Hydrogel for PTT

Schematic illustration of CuS-containing hybrid hydrogel for bacteria killing and acceleration of wound healing under 808 nm NIR. Reproduced with permission from Li et al.[64] Copyright 2018, Royal Society of Chemistry.

performance. Their results disclosed the high binding affinity of CNTs to bacteria and their inherent NIR responsiveness. Since then, high photothermal disinfection efficiencies have been investigated in GO, reduced GO (rGO), carbon quantum dots (CQDs), and graphene quantum dots (GQDs). To date, these carbon-based nanomaterials and their derivatives are still being widely researched and applied in PTT.[52,89,90] For example, Yu et al.[91] developed GQD-Ag NP hybrids for antimicrobial therapy. Compared with GQDs alone, the conjugation of Ag NPs significantly improved the light-heat transformation efficiency under 450 nm of light irradiation. At the same time, there was a remarkable increase in ROS yield. Hence, the GQD-Ag NP hybrids exhibited remarkable bactericidal capability against both *E. coli* and *S. aureus*.

Although the nanomaterials mentioned above have satisfactory photothermal properties, they still have disadvantages—biodegradation difficulty, long-term cytotoxicity, and other side effects. With this in mind, organic PTAs, as candidates for photothermal nanomaterials, are attracting increasing attention, including indocyanine green (ICG),[67] polypyrrole,[92] polyaniline (PANI).[93] In general, after being excited by photons produced by NIR irradiation, organic PTAs absorb energy, rapidly convert to the lowest excited singlet state, and then return to the ground state by generating photons (fluorescence) or non-radiative relaxation pathways. The PTT mechanism triggered by organic PTAs is mainly related to non-radiative relaxation pathways, which requires materials to have a low fluorescence quantum yield and singlet oxygen generation yield, thereby ensuring maximum energy-heat

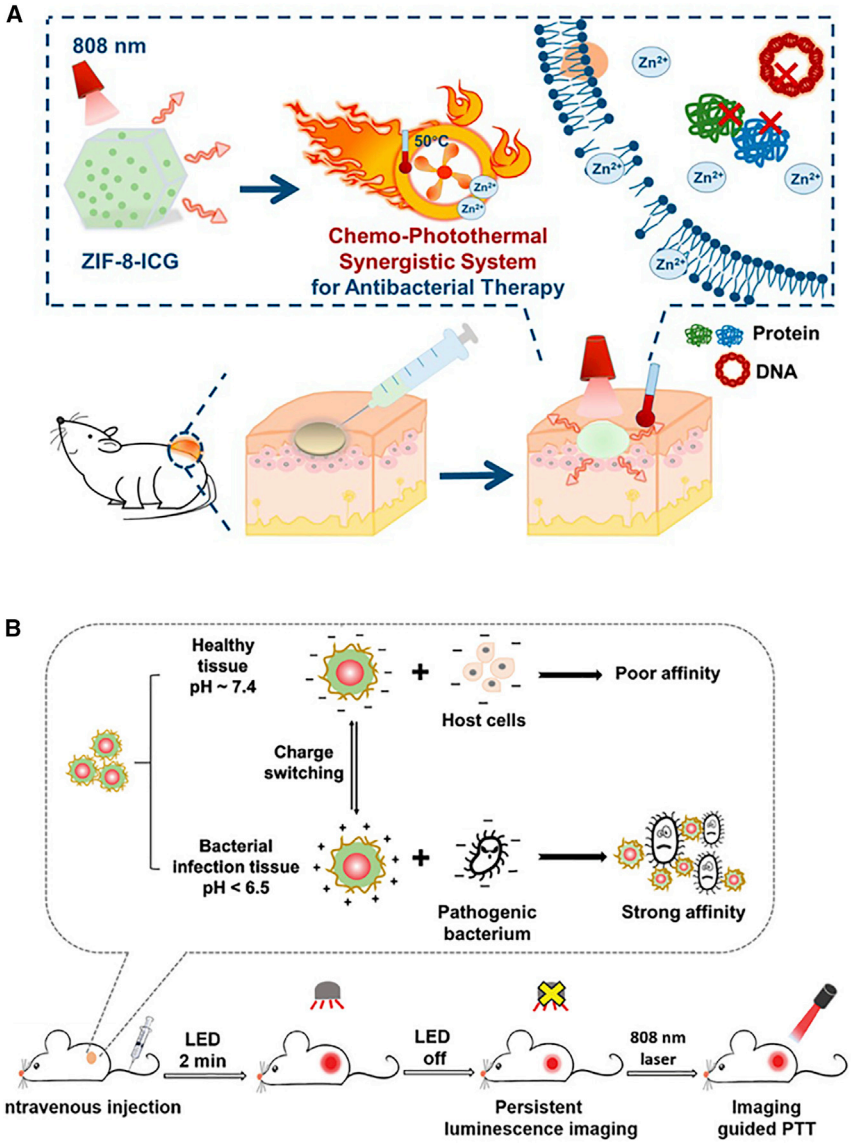

Figure 10. Photothermal Platform Based on Organic PTAs

(A) Schematic illustration of Zn^{2+} assisted ZIF-8-ICG system used for the therapy of MRSA infection using 808 nm. Reproduced with permission from Wu et al.[95] Copyright 2019, MDPI.

(B) Schematic illustration of pH-dependent platform composed of PANI and GCS for imaging-guided and precise PTT. Reproduced with permission from Yan et al.[97] Copyright 2020, John Wiley-VCH & Sons.

conversion.[87] Taking ICG as an example, as it is an amphiphilic cyanine dye, it has strong NIR (600–950 nm) absorption features by a π conjugate system for inducing the PDT and PTT effect, following poor singlet oxygen yield and high heat generation.[94] Wu et al.[95] combined ZIF-8 with ICG to successfully create a synthetic ZIF-8-ICG MOF system, which could thoroughly ablate MRSA (nearly 100% bactericidal ratio) under 808 nm irradiation due to efficient photothermal sterilization from ICG and inhibiting bacterial growth from released Zn^{2+} ions (Figure 10).

Another popular organic PTA, PANI, has also shown great potential for bacteria ablation due to its high photothermal conversion property, its great photostability,

and, most important, its pH-dependent photothermal feature. To be specific, the light-heat conversion property of PANI is much stronger under acidic conditions than under neutral or alkaline conditions.[96] Yan el al.[97] manufactured an intelligent and precise antibacterial nanoplatform based on the pH-dependent photothermal feature of PANI and the pH-responsive surface charge conversion property of glycol chitosan (GCS). As shown in Figure 10, the pH of a normal physiological region is ~7.4, while the pH of infected tissue is <6.5. Therefore, PANI could selectively act on pathological tissues without damaging nearby normal tissues. GCS could also make the acidic bacterial infection positions become positively charged, without influencing the charge of healthy cells, thus helping the platform capture bacteria more precisely. The platform could, therefore, achieve targeted and efficient sterilization and bring little harm to normal tissues, killing >99% of *S. aureus*, *E. coli*, and MRSA under 808 nm irradiation.

Natural Materials as PTAs

Nature is a huge treasure trove of materials, so some researchers have shifted their gaze toward developing natural components into PTAs. This is a promising initiative due to the wide availability, low cost, strong biocompatibility, and negligible cytotoxicity of natural materials. Through extraction, purification, and further processing, various novel and satisfactory photoresponsive antibacterial platforms have been created from natural materials. For example, melanin-like nanomaterials, which can be obtained from human hair, cuttlefish ink, black sesame seeds, and so forth, are considered to be versatile and powerful PTAs with broad biomedical applications. In recent work by the present authors' research team, negatively charged, human hair melanosome derivatives (HHMs) were successfully extracted with the low-temperature alkali heat method and were then combined, through electrostatic interaction, with positively charged lysozyme (Lyso) to form HHMs-Lyso composites.[72] *In vitro* tests proved that the HHMs-Lyso possessed excellent photothermal conversion properties, photothermal reversibility, and cycling stability, and *in vivo* tests confirmed its high antibacterial efficacy against MRSA. In addition, polydopamine (PDA) NPs have the same precursor molecules and similar oxidation-polymerization processes with eumelanin; thus, they are known as melanin-like materials and are being widely explored for biomedical applications.[98]

PTT-Based Synergistic Antibacterial System

Normal tissue caused by local hyperthermia and the unsatisfactory penetration depth of NIR light are two main obstacles inhibiting PTT effects.[99,100] Obviously, single PTT is not ideal for combating bacteria. To solve these questions, PTT is usually synergized with various other antibacterial strategies for sterilization (e.g., metal ion release, drug release, electrostatic adsorption bacteria). Through these well-designed synergistic therapies, treatment time has been shortened, and the sterilization effect has been greatly improved.

Some metal ions, such as Ag^{+}, Cu^{2+}, Zn^{2+}, and Au^{2+},[101] have shown antibacterial properties by interacting with DNA, changing membrane permeability, desaturating proteins, and disrupting intracellular metabolism.[102] Hence, PTT has been widely incorporated with metal ions to achieve a higher sterilization efficiency. Local heat triggered by PTAs can accelerate the release and penetration of ions into bacteria, thus eliminating the bacteria. For example, Cu^{2+} was doped into MoS_2 nanoflowers,[103] where it improved the separation of the electron-hole pairs, promoted ROS production, and enhanced the photothermal effect of MoS_2 due to its d-d transition. An interesting discovery was that Cu^{2+} could also facilitate the oxidation of glutathione in the bacteria, being reduced to Cu^{+} itself, which could act with

H_2O_2 to generate •OH and thereby lessen the bacterial resistance to the surrounding environment. Owing to the combined effects of heat, ROS, and released Cu^{2+}, the designed material exhibited an excellent bacteria-killing efficacy of 99.64% against *S. aureus* under 660 nm irradiation. However, it should be noted that the dosages off metal ions must be controlled, since large concentrations may cause cytotoxicity.[104] Compared with other antibacterial elements, Zn is a good compromise between antibacterial properties and cytotoxicity. Yang et al.[105] modified the Ti surface with a bilayer film, consisting of gold nanorods (GNRs) as the inner layer and PDA containing Zn (PDA@Zn) as the outer layer. When the Zn ions released from the outer layer came into contact with the bacteria, they were absorbed into the bacterial membrane and destroyed the membrane's stability and permeability. When the coating was irradiated with NIR, GNRs could also induce high temperatures and accelerate Zn^{2+} release. As the concentration increased, Zn ions could enter the bacterial cells, interacting with nucleic acids, inhibiting glycolysis, and reducing acid tolerance. Thus, the composite coating possessed both contact and heat-responsiveness-release antibacterial properties against *E. coli* and *S. aureus*.

In addition to being synergized with metal ion release, PTT has also been widely incorporated with drugs to slowly release them, shorten treatment time, and enhance the drugs' therapeutic effects.[106] For example, Ma et al.[107] prepared an antibacterial coating on Ti implants by loading the gentamicin (Gent) with polyethylene glycol (PEG)-modified MoS_2, finally covering it with CS (Figure 11). As a broad-spectrum antibacterial agent with good thermal stability, Gent is well suited to synergy with PTT. When the coating was radiated with 808 nm of light, the increased temperature accelerated Gent release and promoted its entry into the bacteria interiors. With the irradiation of 808 nm of light for a short time, the composite coating achieved a high efficiency of *in situ* sterilization, with antibacterial rates of 99.93% and 99.19% against *E. coli* and *S. aureus*, respectively. Similarly, Wang et al.[108] modified Au nanostars (NSs) with low-concentration vancomycin (Van). As shown in Figure 11, the designed Au NSs displayed a strong absorption in the NIR region due to the LSPR phenomenon and the ability of Van to selectively recognize G^+. Therefore, the platform could target and kill MRSA via the antibacterial ability of Van and the assistance of heat produced under NIR irradiation. In another piece of research,Tan et al.[109] noted that a low-temperature antibacterial platform based on RPNPs and conventional aminoglycoside antibiotics was developed. Different from previous photothermal systems, this platform processed at a mild temperature (45°C), which was not lethal to antibiotic-resistant pathogens. However, the increased temperature could have weakened the activities of many proteins, which may participate in the resistance processes of invalidating antibiotics. By this means, MRSA was re-sensitized to conventional aminoglycoside antibiotics. This work proved that low-temperature antibacterial strategies may have the potential to be exogenous-modifying enzyme inhibitors for dealing with multiple drug-resistant pathogens and prolonging the lives of old antibiotics.

To better enhance disinfection efficacy, the more effective the contact of the light-responsive materials with the bacteria, the better the sterilizing effect. Among the many ways of targeting and capturing bacteria, electrostatic adsorption is the most common.[110,111] The bacterial surface is negatively charged and, therefore, it is easier for positively charged materials to target bacteria[112]—for example, metal ions, polyethyleneimine,[113] GCS,[114] some amino groups.[72] It is worth noting that the process of electrostatic adsorption may be affected by the surrounding physiological environments, such as pH, proteins, temperature, and salt ions.[110] As a typical example, Mei et al.[115] prepared amino-functionalized GO (GO-NH_2), whose

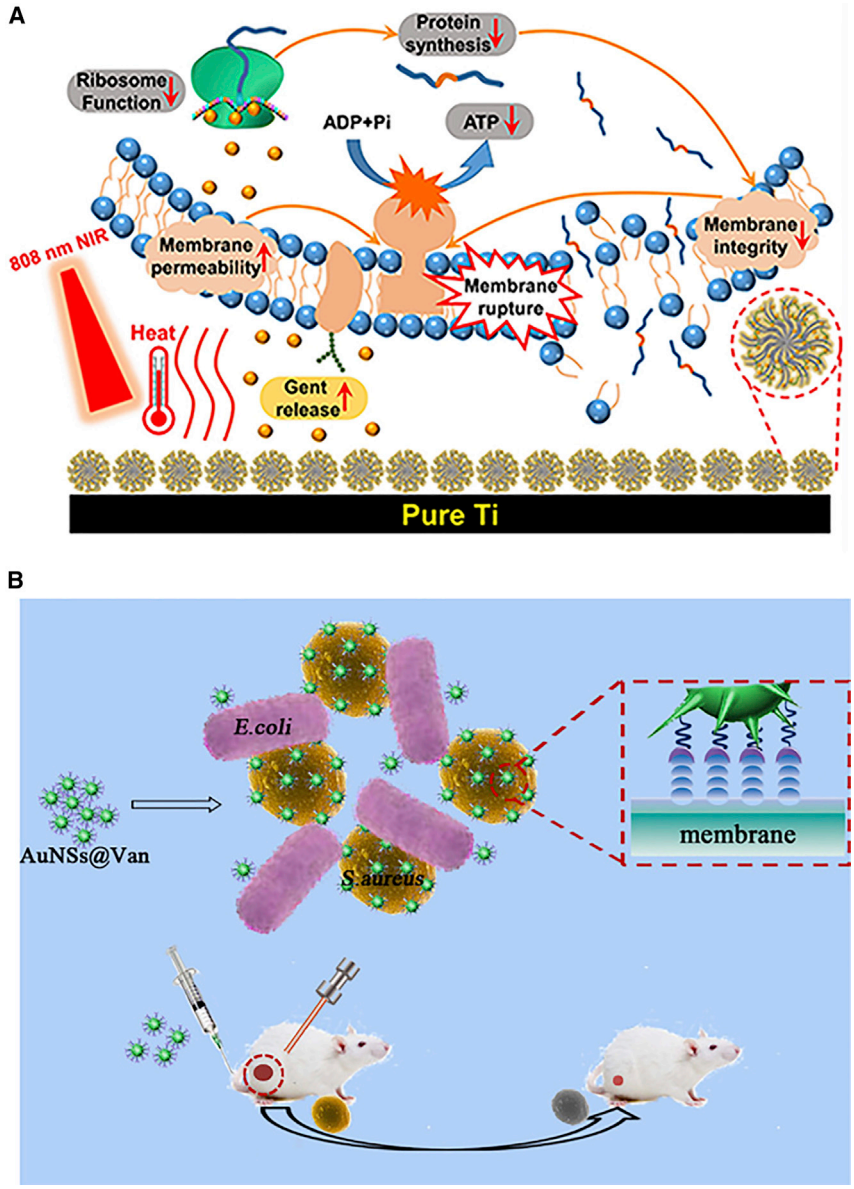

Figure 11. Antibacterial Platform Combined PTT with Drug Release

(A) Schematic illustration of the multiple high-efficiency antibacterial coating based on photothermal and Gent release. Reproduced with permission from Ma et al.[107] Copyright 2019, Royal Society of Chemistry.

(B) Schematic illustration of Au NSs@Van for targeting and killing MRSA under 808 nm irradiation. Reproduced with permission from Wang et al.[108] Copyright 2019, American Chemical Society.

antibacterial activity upon white light was increased by 32 times compared with GO alone. Their results proved that the designed GO-NH_2 could accumulate on bacterial surfaces through electrostatic attraction and effectively damage cell membranes through enhanced photothermal performance, resulting in cytoplasmic leakage to sterilization. In another work, He et al.[116] synthesized a comprehensive system to combine photothermal, drug release, and electrostatic adsorption with bacteria using PDA, GNRs, GCS, and daptomycin (DAP). As shown in Figure 12, they synthesized a PDA coating on GNRs, grafted it with GCS, and finally loaded DAP onto the PDA coating. In the low pH environment of the bacterial infection sites, the

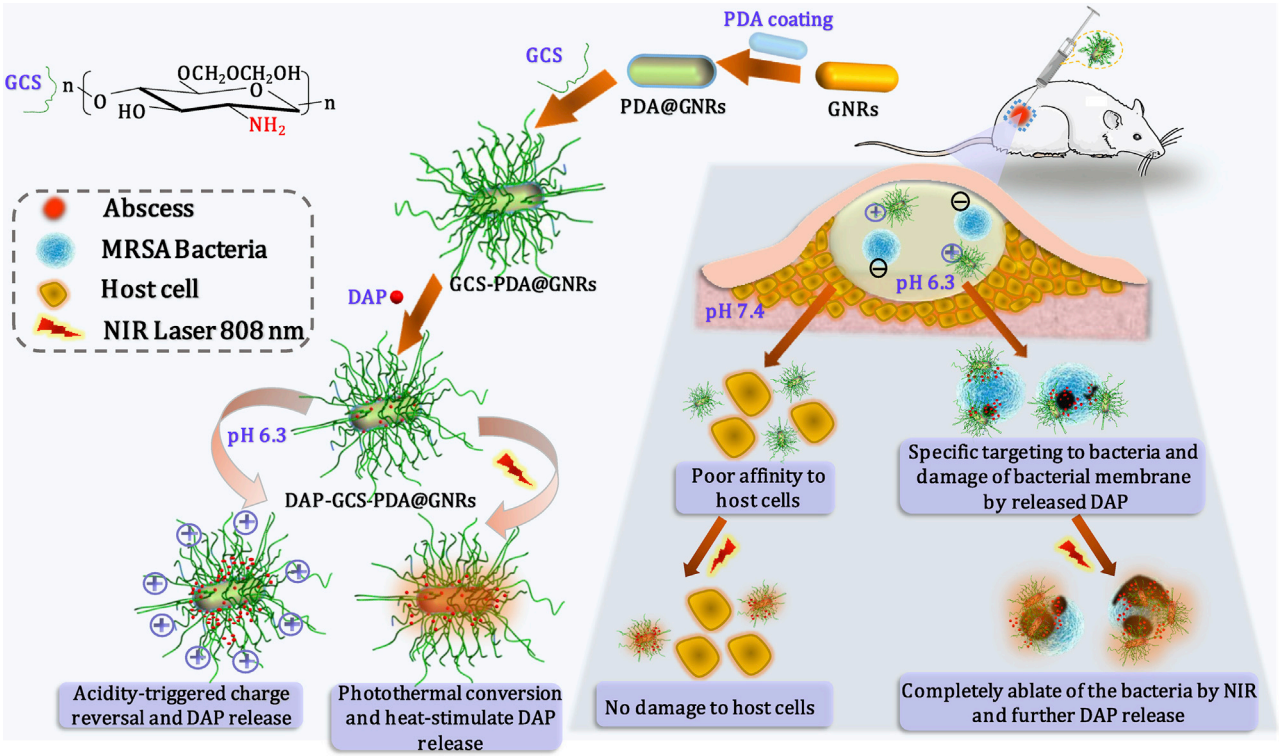

Figure 12. Antibacterial Platform Combining PTT with Antibiotic

Schematic illustration of the preparation processes and antibacterial mechanisms of DAP-GCS-PDA@GNRs based on photothermal and antibiotic. Reproduced with permission from He et al.[116] Copyright 2018, Elsevier BV.

composite coating became positively charged due to the unique property of GCS, ensuring that it targeted the infection site accurately through electrostatic attraction. GNRs and DAP could thus kill the bacteria through PTT and antibiotic therapy simultaneously. Finally, the bacteria inactivation efficiency of the coating against MRSA reached ~100% under 808 nm irradiation.

Chemotherapy for microbial inactivation still presents some disadvantages, especially the inability to avoid promoting bacterial resistance. Compared with chemotherapy, causing physical damage to bacteria will not further bacterial resistance because it offers the bacteria no time to develop specific recognition and active targets. In addition to PTT causing bacterial death through overheating, physical damage also involves physical cutting,[117] magnetic responses,[59] and so forth.

Benefiting from sharp edges, which look like needles or blades, graphene-like 2D materials, acting as nanoknives, can incise or pierce microbial cellular membranes, causing the intracellular substances to leak away and eventually leading to bacterial death.[118,119] Fan et al.[120] integrated ZIF-8 with graphene and obtained ZnO-doped C on graphene (ZnO@G). Then, they grafted the phase-size transformable thermal-responsive brushes (TRBs) onto the ZnO@G to fabricate the TRB-ZnO@G nanocomposite, realizing localized multiple bacterial eradication therapies. NIR-triggered photothermal, localized massive Zn^{2+} penetration, and physical cutting synergistically disrupted bacterial membranes and intracellular substances. The antibacterial experiment results showed that the bactericidal efficiency of the synergistic system against both *E. coli* and *S. aureus* reached nearly 100% in a short time, without accumulating toxicities or damaging normal tissues.

Magnetic response nanomaterials play a unique and ingenious role in inactivating microorganisms due to their special magnetic properties.[121] This feature is used for multiple applications under external magnetic fields, such as magneto-thermal drug release, magnetic release, magnetic separation, and precision targeting.[59,122,123] Yu et al.[124] designed a multifunctional, versatile antibacterial system based on photothermal and nitric oxide (NO) release. PDA coated Fe_3O_4 was synthesized as the core, exhibiting both photoconversion efficiency and superparamagnetic properties. Then, dendritic poly(amidoamine) (PAMAM) and N-diazeniumdiolate (NONOate) were sequentially grafted onto the Fe3O4@PDA surface, obtaining versatile Fe_3O_4@PDA@PAMAM@NONOates nanocomposites. This nanoplatform possessed multiple functions: (1) capturing bacteria via the positively charged surface; (2) killing bacteria via the PTT effect of PDA and NO release; (3) ensuring the photocontrol of NO release via photo-heat conversion; and (4) separating dead bacteria with the external magnetic field.

Synergistic Systems Based on PTT and PDT

Both PTT and PDT have disadvantages when used alone. The high temperatures necessary for PTT may burn healthy tissues.[125] In addition, it is difficult for infected tissues to absorb the NIR preferred for PTT. In PDT, using UV-vis irradiation *in vivo* may also damage some healthy biological tissues.[64] Therefore, many synergistic antibacterial systems combining PTT and PDT have been developed in recent years. In these systems, ROS can increase the permeability and thermal sensitivity of damaged bacterial membranes. Therefore, the sterilization temperature need not reach levels at which it would scald normal tissues. Meanwhile, membrane permeability is also increased with temperature, thus strengthening the therapeutic effect of ROS by accelerating the leakage of proteins and other contents from the bacteria. The following section mainly discusses these synergistic photoresponsive antibacterial systems according to different light sources.

Full-spectrum Responsive Synergistic Antimicrobial System

Solar energy is advantageous because it is abundant and convenient; therefore, it is suitable as the stimulation source for photoresponsive materials. Solar light can be used to simultaneously trigger PDT and PTT because of its wide wavelength range covering UV, visible light, and NIR. To take advantage of the full solar spectrum, it is wise to design composite materials that can both boost ROS generation and convert solar energy to heat. For example, fibrous RP is not only an important semiconductor but also a non-negligible solar photothermal material. Hence, a fibrous RP/ZnO heterojunction thin film was deposited on a Ti substrate to achieve rapid disinfection through ROS-heat synergy.[9] In the platform, the RP/ZnO heterojunction showed a speedy migration of charge carriers, a narrow band gap, and intensive optical absorption, endowing the system with strong photocatalytic performance. Fibrous RP also gave the system excellent sunlight-heat conversion efficiency (>50°C in 2 min). Many solar radiation photons have a greater amount of energy than the RP energy band. Therefore, under exposure to sunlight, the excited carriers are above the band gap, and they can transform the extra energy into heat via a thermalization course.

Synergistic Antimicrobial System Driven by Single-Wavelength Light

As mentioned above, NIR is more suitable for deep treatment than simulated solar light. Therefore, many synergistic photoresponsive systems can also be excited by NIR. For example, a Ti plate with Ag-loaded MoS_2 was immersed in a CS solution to obtain a 660-nm-driven CS/Ag/MoS_2 antibacterial coating (Figure 13).[63] As

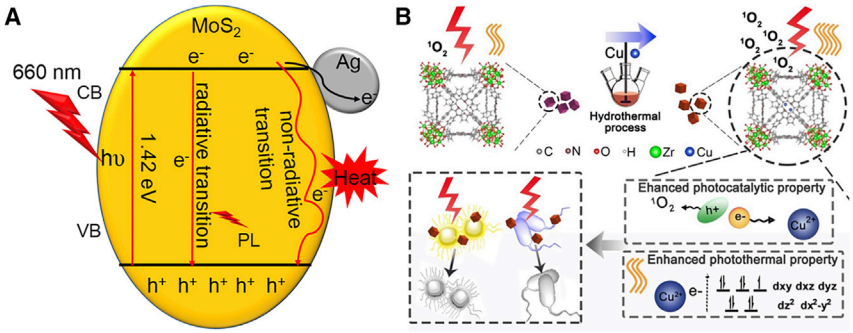

Figure 13. Synergistic Photoresponsive Systems Using 660 nm Irradiation

(A) Schematic illustration of enhanced photocatalytic and photothermal performances of CS/Ag/MoS_2 antibacterial coating. Reproduced with permission from Zhu et al.[63] Copyright 2020, Elsevier BV.

(B) Schematic illustration of preparation procedures and enhanced bacteria-killing properties of Cu-doped MOFs. Reproduced with permission from Han et al.[126] Copyright 2020, Elsevier BV.

mentioned before, MoS_2 possesses both a satisfactory photodynamic effect and prominent photothermal performance. As a result, in this system, the CS/AgMoS_2 coating not only strongly responded to UV-vis light but also harvested NIR, producing ROS and heat to kill bacteria. Under exposure to a 660-nm laser, the coating's antibacterial efficiency toward *E. coli* reached up to 99.77% in 20 min.

In addition, many PSs and PSs-containing materials are used as a matrix to design synergistic photoresponsive platforms. For example, Han et al.[126] introduced a proper amount of Cu^{2+} into PCN-224, a kind of porphyrin-containing MOF. As illuminated in Figure 13, the d-d transition of Cu^{2+} played an important role in strengthening light absorption. Meanwhile, Cu^{2+} hindered the recombination of h^+-e^- pairs. With the existence of porphyrin and the assistance of Cu^{2+}, the synthetized Cu-doped MOFs produced considerable amounts of ROS and translated the light into heat when triggered by 660 nm of light, exhibiting powerful PDT and PTT effects.

Many synergistic antimicrobial platforms have also been developed to respond to another frequently used NIR resource: an 808-nm laser.[127] In one work, a negatively charged RP film was deposited on the Ti surface and immobilized with positively charged IR780, a common PS. Then, the coating was modified with PDA, aiming to enhance the RP photothermal conversion efficiency.[128] PDA includes highly reactive catechol groups, so it inherently possessed an antiseptic function. Owing to the outstanding photocatalytic and photothermal performances of BP, along with the assistance of IR780 and PDA in strengthening the photocatalytic and photothermal properties, respectively, the *in vivo* tests disclosed that the temperature of the implant site increased to 50°C after only 2 min of 808 nm laser irradiation at an intensity of 2.0 W/cm^2. The generation of $^1O_2$ from IR780 showed no differences with the variable temperature; in other words, the temperature had no adverse effect on IR780 photocatalysis. After 10 min of irradiation at 50°C, the system eradicated 96.2% of *S. aureus* on bone implants due to the synergistic effects of both PTT and PDT.

Synergistic Antimicrobial System Driven by Dual Lights

On some occasions, single-wavelength light sources may be not enough to concurrently induce photothermal conversion and ROS generation. Dual-light sources are a

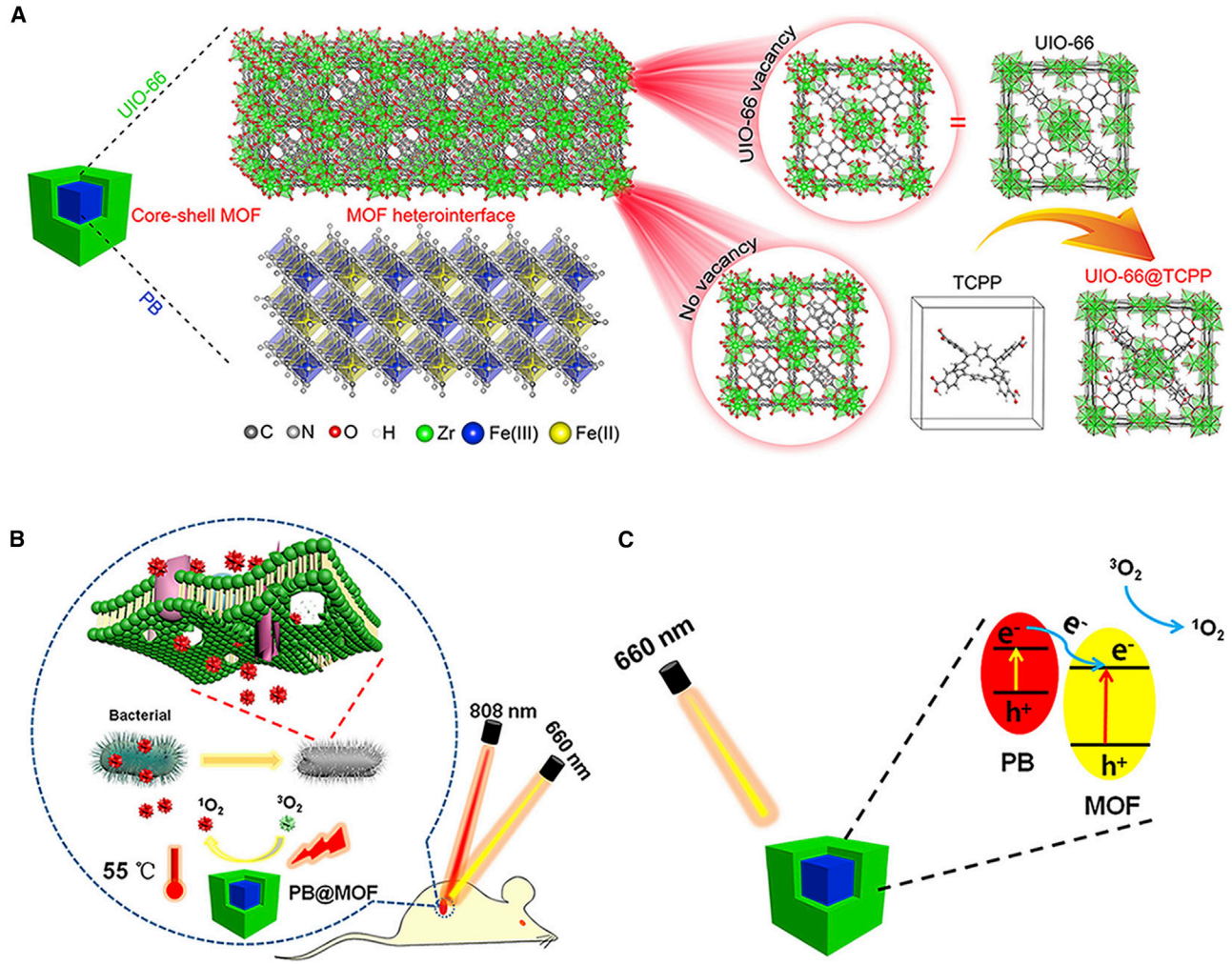

Figure 14. PB@MOF for Synergistic Bacteria Killing

(A) Schematic illustration of the core-shell structure of PB@MOF. Reproduced with permission from Luo et al.[129] Copyright 2019, American Chemical Society.

(B) Schematic illustration of the bacteria killing processes under dual-light irradiation. Reproduced with permission from Luo et al.[129] Copyright 2019, American Chemical Society.

(C) Schematic illustration of the photocatalytic mechanism of PB@MOF Heterojunction. Reproduced with permission from Luo et al.[129] Copyright 2019, American Chemical Society.

reasonable solution.[90,129] In one work, a core-shell dual MOF (PB@MOF) was synthesized, with PB acting as the core and porphyrin-doped UIO-66 as the shell (Figure 14).[129] When exposed to 660 nm of light, the synthesized PB@MOF showed satisfactory yields of $^1O_2$. PB accelerated the separation and migration of the photogenerated carriers, while 808 nm cannot trigger the photocatalytic activity of PB@MOF. However, PB@MOF showed no photothermal effect under 660 nm irradiation. These results indicated that 660 nm irradiation could only trigger the photocatalytic process, and 808 nm irradiation could only drive the photothermal process. Furthermore, mixing light was the motivation for this antibacterial platform. Under the irradiation of dual lights, the dual MOF concurrently exhibited a high photothermal conversion efficiency and rapid generation of $^1O_2$. It is, therefore, not surprising that within 10 min, the designed PB@MOF achieved high antibacterial efficacies of 99.31% and 98.68% against *S. aureus* and *E. coli*, respectively.

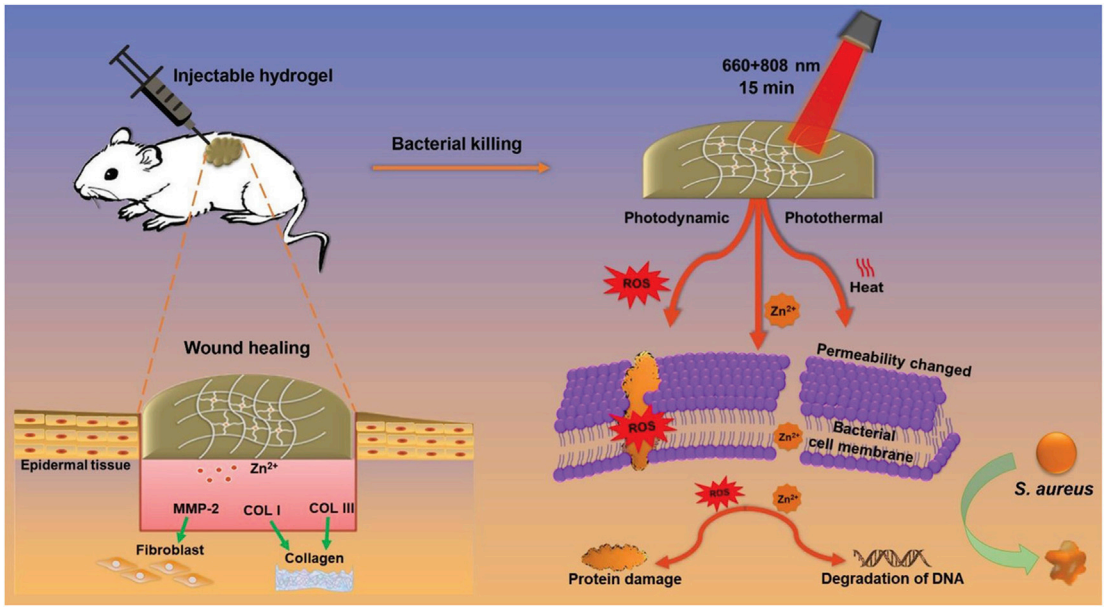

Figure 15. DFT-C/ZnO-Hydrogel for Synergistic Bacteria Killing

Schematic illustration of DFT-C/ZnO-hydrogel for killing bacteria and promoting wound healing under dual-light irradiation. Reproduced with permission from Xiang et al.[90] Copyright 2019, John Wiley-VCH & Sons.

PDT- and PTT-Based Multiple Synergy

The above-mentioned synergistic, photoresponsive platforms involve PDT and PTT acting together. However, there are also some multiple antibacterial systems that combine PDT and PTT with other mechanisms to combat microbes.

For example, an injectable antibacterial hydrogel was synthesized by binding PDA and folic acid (FA) with Zn^{2+} and loading CQD-decorated ZnO (C/ZnO) NPs with PDA (Figure 15).[90] The up-conversion effect of the CQDs enhanced the ROS generation of the ZnO. The prepared hydrogel reached up to 55°C within 15 min under the illumination of 660 and 808 nm of light because both PDA and CQDs could produce heat. Meanwhile, the hydrogel released Zn^{2+} over 12 days, resulting in a long-lasting antibacterial effect and promoting fibroblast proliferation. What is more, the PDA endowed the antibacterial hydrogel with tissue adhesion, hemostatic ability, and self-healing ability. Above all, this hybrid hydrogel exhibited great potential for healing bacteria-infected wounds and reconstructing tissues, especially for irregular wounds, because it could perfectly match the wound shape.

Summary and Outlook

The development of photoresponsive materials and platforms for microbial inactivation has attained tremendous achievements in recent years, and Table 1 summarizes the representative photoresponsive antibacterial materials. Compared to traditional antibiotics, PDT and PTT can effectively treat inflammation and infection in a short time, without invasiveness or side effects, and, most important, they do not encourage bacterial resistance. Constructing antibacterial coatings on the surface of biomedical implants and biomedical devices can reduce the risk of postoperative infections, and photoactivated antibacterial dressings can both eliminate infection and promote wound healing. In addition, the newly developed technology can be applied to touch screen sterilization, water disinfection, and many other fields.[130]

Table 1. Summary of Photoresponsive Systems for Microbial Inactivation

Photoresponsive Components	PDT or PTT	Light Source	Biocides	Microorganism	Ref.
RP/ZnO nanofilm	PDT and PTT	solar light, LED	Zn^{2+}	*E. coli*, *S. aureus*	9
g-C_3N_4	PDT	visible light		*E. coli*	22
g-C_3N_4-Zn^{2+}@GO	PDT and PTT	808 and 660 nm	Zn^{2+}	*E. coli*, *S. aureus*	23
MnO_2/g-C_3N_4	PDT	visible light		*E. coli*, *S. aureus*	27
TiO_2-Bi_2WO_6 binanosheets	PDT	visible light		*E. coli*	29
Halogenated porphyrin Zn derivatives@TiO_2	PDT	visible light		*E. coli*, *S. aureus*	39
ZnO-TSPP	PDT	visible light		*E. coli*, *S. aureus*	40
Ag/AgBr	PDT	solar light	Ag^+	*E. coli*, *S. aureus*	44
Porphyrin@Ag NPs	PDT	LED	Ag^+	*E. coli*, *S. epidermidis*	45
Au@Bi_2WO_6 nanosheets		808 nm	Au^+	*E. coli*, *S. aureus*	46
Er and Ce co-doped TiO_2	PDT	visible light		*E. coli*, *S. aureus*	47
$NaYF_4$: Er/Yb/Mn@MB)	PDT	980 nm		MDR *E. coli*, MDR *S. aureus*	48
Ag_3PO_4/GO	PDT	660 nm	Ag^+	*E. coli*, *S. aureus*	52
BP nanosheets	PTT	visible light	CS	*E. coli*, *S. aureus*	55
Triangular Ag NPs	PTT	808 nm	Ag^+	EBSL *E. coli*, MRSA	59
Au-Ag NPs	PTT	808 nm	Au^+ and Ag^+	*E. coli*, *S. aureus*	60
Ag/MoS_2	PDT and PTT	660 nm	CS and Ag^+	*E. coli*, *S. aureus*	63
CuS	PDT and PTT	808 nm	Cu^{2+}	*E. coli*, *S. aureus*	64
Hair-melanosome derivatives	PTT	808 nm	lyso	MRSA	72
ZnPB	PDT and PTT	808 nm	Zn^{2+}, Fe^{2+}, and Fe^{3+}	*E. coli*, MRSA	80
HuA@ZIF-8	PTT	808 nm	Zn^{2+}	*E. coli*, *S. aureus*	81
PB	PTT	808 nm	CS	*E. coli*, *S. aureus*	82
CuS@MoS_2	PDT and PTT	808 and 660 nm		*E. coli*, *S. aureus*	86
CQDs/ZnO	PDT and PTT	808 and 660 nm	Zn^{2+}	*E. coli*, *S. aureus*	90
GQD-Ag NPs	PDT and PTT	450 nm	Ag^+	*E. coli*, *S. aureus*	91
ZIF-8-ICG	PTT	808 nm	Zn^{2+}	MRSA	95
PANI	PTT	808 nm	GCS	*E. coli*, *S. aureus*, MRSA	97
Cu-doped MoS_2	PDT and PTT	660 nm	Cu^{2+}	*S. aureus*	103
GNRs	PTT	808 nm	Zn^{2+}	*E. coli*, *S. aureus*	105

(*Continued on next page*)

Table 1. *Continued*

Photoresponsive Components	PDT or PTT	Light Source	Biocides	Microorganism	Ref.
MoS_2	PTT	808 nm	Gent and CS	*E. coli*, *S. aureus*	107
Au nanostars	PTT	808 nm	Van	*E. coli*, MRSA	108
RP	PTT	808 nm	Gent	MRSA	109
GO-NH_2	PTT	solar light		*E. coli*	115
GNRs	PTT	808 nm	DAP and GCS	MRSA	116
ZnO@G	PTT	808 nm	Zn^{2+}	*E. coli*, *S. aureus*	120
Fe_3O_4@PDA	PTT	808 nm	NO	*E. coli*, *S. aureus*	124
Cu-doped PCN 224	PDT and PTT	660 nm	Cu^{2+}	*E. coli*, *S. aureus*	126
RP-IR 780-PDA	PDT and PTT	808 nm	–	*E. coli*, *S. aureus*	128
PB@UIO-66-TCPP	PDT and PTT	808 and 660 nm	–	*E. coli*, *S. aureus*	129

Even though these achievements, as reviewed above, are impressive, it should be emphasized that some challenges remain. Although various bacteria platforms have been reported, most of them are proofs of concepts, and some models could only be fabricated under laboratory conditions due to the sophisticated preparation processes and complex usage procedures. Therefore, simple, economical, practical, convenient, and reproducible materials and therapies should be given more attention in future studies.[131] Despite solving the problem of drug resistance, the required dosage of photoresponsive materials is much higher than that of antibiotics, and most current photoresponsive materials are nondegradable, so cytotoxicity must be emphasized. In addition, the phototoxicity of light sources, which may damage normal tissues, has not yet received enough attention. In future research, optimizing materials' photoresponsive abilities to reduce the required intensity of the excitation source will be the most effective solution. Finally, the present authors hope that this review will inspire more researchers to follow this path of study and develop promising photoresponsive materials for antibacterial applications.

ACKNOWLEDGMENTS

This study was jointly supported by the National Science Fund for Distinguished Young Scholars (no. 51925104), the National Natural Science Foundation of China (nos. 51671081 and 51871162), the Natural Science Fund of Hubei Province (no. 2018CFA064), RGC/NSFC (N_HKU725-1616), Hong Kong ITC (ITS/287/17, GHX/002/14SZ), and the Health and Medical Research Fund (no. 03142446).

AUTHOR CONTRIBUTIONS

Supervision, X.L. and S.W.; Conceptualization, X.L., Y.Z., Z.L, C.L, K.W.K.Y., and S.W.; Visualization, X.L., Y.R., H.L., and S.W.; Writing—Original Draft, Y.R. and H.L.; Writing—Review and Editing, X.L., Z.L., S.Z., Y.L., Z.C., and S.W.

DECLARATION OF INTERESTS

The authors declare no competing interests.

REFERENCES

1. Perry, R.D., and Fetherston, J.D. (1997). Yersinia pestis–etiologic agent of plague. Clin. Microbiol. Rev. *10*, 35–66.
2. Bos, K.I., Schuenemann, V.J., Golding, G.B., Burbano, H.A., Waglechner, N., Coombes, B.K., McPhee, J.B., DeWitte, S.N., Meyer, M., Schmedes, S., et al. (2011). A draft genome of Yersinia pestis from victims of the Black Death. Nature *478*, 506–510.
3. Levy, S.B., and Marshall, B. (2004). Antibacterial resistance worldwide: causes, challenges and responses. Nat. Med. *10* (12, Suppl), S122–S129.
4. Mendelson, M., and Matsoso, M.P. (2015). The World Health Organization Global Action Plan for antimicrobial resistance. S. Afr. Med. J. *105*, 325.
5. Alanis, A.J. (2005). Resistance to antibiotics: are we in the post-antibiotic era? Arch. Med. Res. *36*, 697–705.
6. Wei, T., Yu, Q., and Chen, H. (2019). Responsive and synergistic antibacterial coatings: fighting against bacteria in a smart and effective way. Adv. Healthc. Mater. *8*, e1801381.
7. Qiao, Y., Liu, X., Li, B., Han, Y., Zheng, Y., Yeung, K.W.K., Li, C., Cui, Z., Liang, Y., Li, Z., et al. (2020). Treatment of MRSA-infected osteomyelitis using bacterial capturing, magnetically targeted composites with microwave-assisted bacterial killing. Nat. Commun. *11*, 4446.
8. Zhang, T., Lin, H., Cui, L., An, N., Tong, R., Chen, Y., Yang, C., Li, X., and Qu, F. (2016). NIR-sensitive UCNP@mSiO$_2$ nanovehicles for on-demand drug release and photodynamic therapy. RSC Advances *6*, 26479–26489.
9. Li, J., Liu, X., Tan, L., Liang, Y., Cui, Z., Yang, X., Zhu, S., Li, Z., Zheng, Y., Yeung, K.W.K., et al. (2019). Light-activated rapid disinfection by accelerated charge transfer in red phosphorus/ZnO heterointerface. Small Methods *3*, 1900048.
10. Liu, Y., Qin, R., Zaat, S.A.J., Breukink, E., and Heger, M. (2015). Antibacterial photodynamic therapy: overview of a promising approach to fight antibiotic-resistant bacterial infections. J. Clin. Transl. Res. *1*, 140–167.
11. Sun, Y.D., Zhu, Y.X., Zhang, X., Jia, H.R., Xia, Y., and Wu, F.G. (2019). Role of cholesterol conjugation in the antibacterial photodynamic therapy of branched polyethylenimine-containing nanoagents. Langmuir *35*, 14324–14331.
12. Sunada, K., Kikuchi, Y., Hashimoto, K., and Fujishima, A. (1998). Bactericidal and detoxification effects of TiO$_2$ thin film photocatalysts. Environ. Sci. Technol. *32*, 726–728.
13. Applerot, G., Lipovsky, A., Dror, R., Perkas, N., Nitzan, Y., Lubart, R., and Gedanken, A. (2009). Enhanced antibacterial activity of nanocrystalline ZnO due to increased ROS-mediated cell injury. Adv. Healthc. Mater. *19*, 842–852.
14. Duan, G., Chen, L., Jing, Z., De Luna, P., Wen, L., Zhang, L., Zhao, L., Xu, J., Li, Z., Yang, Z., and Zhou, R. (2019). Robust antibacterial activity of tungsten oxide (WO$_{3-x}$) nanodots. Chem. Res. Toxicol. *32*, 1357–1366.
15. Chen, X., Liu, L., and Huang, F. (2015). Black titanium dioxide (TiO$_2$) nanomaterials. Chem. Soc. Rev. *44*, 1861–1885.
16. Yang, B., Chen, Y., and Shi, J. (2019). Reactive oxygen species (ROS)-based nanomedicine. Chem. Rev. *119*, 4881–4985.
17. Chen, X., and Burda, C. (2008). The electronic origin of the visible-light absorption properties of C-, N- and S-doped TiO$_2$ nanomaterials. J. Am. Chem. Soc. *130*, 5018–5019.
18. Fang, W., Xing, M., and Zhang, J. (2017). Modifications on reduced titanium dioxide photocatalysts: a review. J. Photochem. Photobiol. C *32*, 21–39.
19. Chandra, D., and Bhaumik, A. (2008). Super-microporous TiO$_2$ synthesized by using new designed chelating structure directing agents. Microporous Mesoporous Mater. *112*, 533–541.
20. Xiao, F.X. (2012). Construction of highly ordered ZnO-TiO$_2$ nanotube arrays (ZnO/TNTs) heterostructure for photocatalytic application. ACS Appl. Mater. Interfaces *4*, 7055–7063.
21. Wang, X., Maeda, K., Thomas, A., Takanabe, K., Xin, G., Carlsson, J.M., Domen, K., and Antonietti, M. (2009). A metal-free polymeric photocatalyst for hydrogen production from water under visible light. Nat. Mater. *8*, 76–80.
22. Huang, J., Ho, W., and Wang, X. (2014). Metal-free disinfection effects induced by graphitic carbon nitride polymers under visible light illumination. Chem. Commun. (Camb.) *50*, 4338–4340.
23. Li, Y., Liu, X., Tan, L., Cui, Z., Jing, D., Yang, X., Liang, Y., Li, Z., Zhu, S., Zheng, Y., et al. (2019). Eradicating multidrug-resistant bacteria rapidly using a multi functional g-C$_3$N$_4$@Bi$_2$S$_3$ nanorod heterojunction with or without antibiotics. Adv. Healthc. Mater. *29*, 1900946.
24. Tang, Z., Kong, N., Ouyang, J., Feng, C., Kim, N.Y., Ji, X., Wang, C., Farokhzad, O.C., Zhang, H., and Tao, W. (2020). Phosphorus science-oriented design and synthesis of multifunctional nanomaterials for biomedical applications. Matter *2*, 297–322.
25. Zhang, Q., Liu, X., Tan, L., Cui, Z., Yang, X., Li, Z., Liang, Y., Zhu, S., Yeung, K.W.K., Wang, X., et al. (2019). A near infrared-activated photocatalyst based on elemental phosphorus by chemical vapor deposition. Appl. Catal. B *258*, 117980.
26. Low, J., Yu, J., Jaroniec, M., Wageh, S., and Al-Ghamdi, A.A. (2017). Heterojunction Photocatalysts. Adv. Mater. *29*, 1601694.
27. Wu, B., Li, Y., Su, K., Tan, L., Liu, X., Cui, Z., Yang, X., Liang, Y., Li, Z., Zhu, S., et al. (2019). The enhanced photocatalytic properties of MnO$_2$/g-C$_3$N$_4$ heterostructure for rapid sterilization under visible light. J. Hazard. Mater. *377*, 227–236.
28. Hu, J., Chen, D., Mo, Z., Li, N., Xu, Q., Li, H., He, J., Xu, H., and Lu, J. (2019). Z-scheme 2D/2D heterojunction of black phosphorus/monolayer Bi$_2$WO$_6$ nanosheets with enhanced photocatalytic activities. Angew. Chem. Int. Ed. *58*, 2073–2077.
29. Jia, Y., Zhan, S., Ma, S., and Zhou, Q. (2016). Fabrication of TiO$_2$-Bi$_2$WO$_6$ binanosheet for enhanced solar photocatalytic disinfection of *E. coli*: insights on the mechanism. ACS Appl. Mater. Interfaces *8*, 6841–6851.
30. Jia, H.R., Zhu, Y.X., Chen, Z., and Wu, F.G. (2017). Cholesterol-assisted bacterial cell surface engineering for photodynamic inactivation of gram-positive and gram-negative bacteria. ACS Appl. Mater. Interfaces *9*, 15943–15951.
31. Calixto, G.M.F., Bernegossi, J., de Freitas, L.M., Fontana, C.R., and Chorilli, M. (2016). Nanotechnology-based drug delivery systems for photodynamic therapy of cancer: a review. Molecules *21*, 342.
32. Ethirajan, M., Chen, Y., Joshi, P., and Pandey, R.K. (2011). The role of porphyrin chemistry in tumor imaging and photodynamic therapy. Chem. Soc. Rev. *40*, 340–362.
33. Josefsen, L.B., and Boyle, R.W. (2012). Unique diagnostic and therapeutic roles of porphyrins and phthalocyanines in photodynamic therapy, imaging and theranostics. Theranostics *2*, 916–966.
34. Fekrazad, R., Ghasemi Barghi, V., Poorsattar Bejeh Mir, A., and Shams-Ghahfarokhi, M. (2015). *In vitro* photodynamic inactivation of Candida albicans by phenothiazine dye (new methylene blue) and Indocyanine green (EmunDo®). Photodiagn. Photodyn. Ther. *12*, 52–57.
35. Beirão, S., Fernandes, S., Coelho, J., Faustino, M.A.F., Tomé, J.P.C., Neves, M.G.P.M.S., Tomé, A.C., Almeida, A., and Cunha, A. (2014). Photodynamic inactivation of bacterial and yeast biofilms with a cationic porphyrin. Photochem. Photobiol. *90*, 1387–1396.
36. Deda, D.K., Uchoa, A.F., Caritá, E., Baptista, M.S., Toma, H.E., and Araki, K. (2009). A new micro/nanoencapsulated porphyrin formulation for PDT treatment. Int. J. Pharm. *376*, 76–83.
37. Wang, C., Li, J., Mele, G., Yang, G.-M., Zhang, F., Palmisano, L., and Vasapollo, G. (2007). Efficient degradation of 4-nitrophenol by using functionalized porphyrin-TiO$_2$ photocatalysts under visible irradiation. Appl. Catal. B *76*, 218–226.
38. Chen, D., Wang, K., Hong, W., Zong, R., Yao, W., and Zhu, Y. (2015). Visible light photoactivity enhancement via CuTCPP hybridized g-C$_3$N$_4$ nanocomposite. Appl. Catal. B *166*, 366–373.
39. Sułek, A., Pucelik, B., Kuncewicz, J., Dubin, G., and Dąbrowski, J.M. (2019). Sensitization of TiO$_2$ by halogenated porphyrin derivatives for visible light biomedical and environmental photocatalysis. Catal. Today *335*, 538–549.
40. Senthilkumar, S., Hariharan, R., Suganthi, A., Ashokkumar, M., Rajarajan, M., and

Pitchumani, K. (2013). Synergistic photodynamic action of ZnO nanomaterials encapsulated meso-tetra (4-sulfonatophenyl) porphyrin. Powder Technol. *237*, 497–505.

41. Hou, W., and Cronin, S.B. (2013). A review of surface plasmon resonance-enhanced photocatalysis. Adv. Funct. Mater. *23*, 1612–1619.

42. Tian, Y., and Tatsuma, T. (2004). Plasmon-induced photoelectrochemistry at metal nanoparticles supported on nanoporous TiO_2. Chem. Commun. (Camb.) *16*, 1810–1811.

43. Le, F., Brandl, D.W., Urzhumov, Y.A., Wang, H., Kundu, J., Halas, N.J., Aizpurua, J., and Nordlander, P. (2008). Metallic nanoparticle arrays: a common substrate for both surface-enhanced Raman scattering and surface-enhanced infrared absorption. ACS Nano *2*, 707–718.

44. Jin, C., Liu, X., Tan, L., Cui, Z., Yang, X., Zheng, Y., Yeung, K.W.K., Chu, P.K., and Wu, S. (2018). Ag/AgBr-loaded mesoporous silica for rapid sterilization and promotion of wound healing. Biomater. Sci. *6*, 1735–1744.

45. Elashnikov, R., Radocha, M., Panov, I., Rimpelova, S., Ulbrich, P., Michalcova, A., Svorcik, V., and Lyutakov, O. (2019). Porphyrin-silver nanoparticles hybrids: synthesis, characterization and antibacterial activity. Mater. Sci. Eng. C *102*, 192–199.

46. Li, B., Tan, L., Liu, X., Li, Z., Cui, Z., Liang, Y., Zhu, S., Yang, X., Kwok Yeung, K.W., and Wu, S. (2019). Superimposed surface plasma resonance effect enhanced the near-infrared photocatalytic activity of $Au@Bi_2WO_6$ coating for rapid bacterial killing. J. Hazard. Mater. *380*, 120818.

47. Ren, Y., Han, Y., Li, Z., Liu, X., Zhu, S., Liang, Y., Yeung, K.W.K., and Wu, S. (2020). Ce and Er Co-doped TiO_2 for rapid bacteria-killing using visible light. Bioact. Mater. *5*, 201–209.

48. Yin, M., Li, Z., Zhou, L., Dong, K., Ren, J., and Qu, X. (2016). A multifunctional upconverting nanoparticle incorporated polycationic hydrogel for near-infrared triggered and synergistic treatment of drug-resistant bacteria. Nanotechnology *27*, 125601.

49. Shrestha, A., and Kishen, A. (2012). The effect of tissue inhibitors on the antibacterial activity of chitosan nanoparticles and photodynamic therapy. J. Endod. *38*, 1275–1278.

50. Zhao, Q., Li, J., Zhang, X., Li, Z., and Tang, Y. (2016). Cationic oligo(thiophene ethynylene) with broad-spectrum and high antibacterial efficiency under white light and specific biocidal activity against *S. aureus* in dark. ACS Appl. Mater. Interfaces *8*, 1019–1024.

51. Jeon, H.J., Yi, S.C., and Oh, S.G. (2003). Preparation and antibacterial effects of Ag-SiO_2 thin films by sol-gel method. Biomaterials *24*, 4921–4928.

52. Xie, X., Mao, C., Liu, X., Tan, L., Cui, Z., Yang, X., Zhu, S., Li, Z., Yuan, X., Zheng, Y., et al. (2018). Tuning the bandgap of photo-sensitive polydopamine/Ag_3PO_4/graphene oxide coating for rapid, noninvasive disinfection of implants. ACS Cent. Sci. *4*, 724–738.

53. Rabea, E.I., Badawy, M.E.T., Stevens, C.V., Smagghe, G., and Steurbaut, W. (2003). Chitosan as antimicrobial agent: applications and mode of action. Biomacromolecules *4*, 1457–1465.

54. Naskar, S., Koutsu, K., and Sharma, S. (2019). Chitosan-based nanoparticles as drug delivery systems: a review on two decades of research. J. Drug Target. *27*, 379–393.

55. Mao, C., Xiang, Y., Liu, X., Cui, Z., Yang, X., Li, Z., Zhu, S., Zheng, Y., Yeung, K.W.K., and Wu, S. (2018). Repeatable photodynamic therapy with triggered signaling pathways of fibroblast cell proliferation and differentiation to promote bacteria-accompanied wound healing. ACS Nano *12*, 1747–1759.

56. Wei, T., Zhan, W., Cao, L., Hu, C., Qu, Y., Yu, Q., and Chen, H. (2016). Multifunctional and regenerable antibacterial surfaces fabricated by a universal strategy. ACS Appl. Mater. Interfaces *8*, 30048–30057.

57. Hanakova, A., Bogdanova, K., Tomankova, K., Pizova, K., Malohlava, J., Binder, S., Bajgar, R., Langova, K., Kolar, M., Mosinger, J., and Kolarova, H. (2014). The application of antimicrobial photodynamic therapy on *S. aureus* and *E. coli* using porphyrin photosensitizers bound to cyclodextrin. Microbiol. Res. *169*, 163–170.

58. Han, D., Ma, M., Han, Y., Cui, Z., Liang, Y., Liu, X., Li, Z., Zhu, S., and Wu, S. (2020). Eco-friendly hybrids of carbon quantum dots modified MoS_2 for rapid microbial inactivation by strengthened photocatalysis. ACS Sustain. Chem. Eng. *8*, 534–542.

59. Qiao, Y., Ma, F., Liu, C., Zhou, B., Wei, Q., Li, W., Zhong, D., Li, Y., and Zhou, M. (2018). Near-infrared laser-excited nanoparticles to eradicate multidrug-resistant bacteria and promote wound healing. ACS Appl. Mater. Interfaces *10*, 193–206.

60. Jiang, X., Fan, X., Xu, W., Zhang, R., and Wu, G. (2020). Biosynthesis of bimetallic Au-Ag nanoparticles using *Escherichia coli* and its biomedical applications. ACS Biomater. Sci. Eng. *6*, 680–689.

61. Lin, L.-S., Cong, Z.-X., Cao, J.-B., Ke, K.-M., Peng, Q.-L., Gao, J., Yang, H.-H., Liu, G., and Chen, X. (2014). Multifunctional Fe_3O_4@polydopamine core-shell nanocomposites for intracellular mRNA detection and imaging-guided photothermal therapy. ACS Nano *8*, 3876–3883.

62. Wang, L., Guan, S., Weng, Y., Xu, S.-M., Lu, H., Meng, X., and Zhou, S. (2019). Highly efficient vacancy-driven photothermal therapy mediated by ultrathin MnO_2 nanosheets. ACS Appl. Mater. Interfaces *11*, 6267–6275.

63. Zhu, M., Liu, X., Tan, L., Cui, Z., Liang, Y., Li, Z., Kwok Yeung, K.W., and Wu, S. (2020). Photo-responsive chitosan/Ag/MoS_2 for rapid bacteria-killing. J. Hazard. Mater. *383*, 121122.

64. Li, M., Liu, X., Tan, L., Cui, Z., Yang, X., Li, Z., Zheng, Y., Yeung, K.W.K., Chu, P.K., and Wu, S. (2018). Noninvasive rapid bacteria-killing and acceleration of wound healing through photothermal/photodynamic/copper ion synergistic action of a hybrid hydrogel. Biomater. Sci. *6*, 2110–2121.

65. Xin, Q., Shah, H., Nawaz, A., Xie, W., Akram, M.Z., Batool, A., Tian, L., Jan, S.U., Boddula, R., Guo, B., et al. (2019). Antibacterial carbon-based nanomaterials. Adv. Mater. *31*, e1804838.

66. Chen, B., Kankala, R.K., Zhang, Y., Xiang, S., Tang, H., Wang, Q., Yang, D.-Y., Wang, S., Zhang, Y.S., Liu, G., et al. (2020). Gambogic acid augments black phosphorus quantum dots (BPQDs)-based synergistic chemo-photothermal therapy through downregulating heat shock protein expression. Chem. Eng. J. *390*, 124312.

67. Fan, H., Fan, Y., Du, W., Cai, R., Gao, X., Liu, X., Wang, H., Wang, L., and Wu, X. (2020). Enhanced type I photoreaction of indocyanine green via electrostatic-force-driven aggregation. Nanoscale *12*, 9517–9523.

68. Han, Y.H., Kankala, R.K., Wang, S.B., and Chen, A.Z. (2018). Leveraging engineering of indocyanine green-encapsulated polymeric nanocomposites for biomedical applications. Nanomaterials (Basel) *8*, 360.

69. Xu, J.W., Yao, K., and Xu, Z.K. (2019). Nanomaterials with a photothermal effect for antibacterial activities: an overview. Nanoscale *11*, 8680–8691.

70. Zhang, X., Xia, L., Chen, X., Chen, Z., and Wu, F. (2017). Hydrogel-based phototherapy for fighting cancer and bacterial infection. Sci. China Mater. *6*, 487–503.

71. Espinosa, A., Reguera, J., Curcio, A., Muñoz-Noval, Á., Kuttner, C., Van de Walle, A., Liz-Marzán, L.M., and Wilhelm, C. (2020). Janus magnetic-plasmonic nanoparticles for magnetically guided and thermally activated cancer therapy. Small *16*, e1904960.

72. Li, J., Liu, X., Zhou, Z., Tan, L., Wang, X., Zheng, Y., Han, Y., Chen, D.F., Yeung, K.W.K., Cui, Z., et al. (2019). Lysozyme-assisted photothermal eradication of methicillin-resistant *Staphylococcus aureus* infection and accelerated tissue repair with natural melanosome nanostructures. ACS Nano *13*, 11153–11167.

73. Xu, D., Li, Z., Li, L., and Wang, J. (2020). Insights into the photothermal conversion of 2D MXene nanomaterials: synthesis, mechanism, and applications. Adv. Funct. Mater. https://doi.org/10.1002/adfm.202000712.

74. Zhao, Y.Q., Sun, Y., Zhang, Y., Ding, X., Zhao, N., Yu, B., Zhao, H., Duan, S., and Xu, F.J. (2020). Well-defined gold nanorod/polymer hybrid coating with inherent antifouling and photothermal bactericidal properties for treating an infected hernia. ACS Nano *14*, 2265–2275.

75. Horcajada, P., Gref, R., Baati, T., Allan, P.K., Maurin, G., Couvreur, P., Férey, G., Morris, R.E., and Serre, C. (2012). Metal-organic frameworks in biomedicine. Chem. Rev. *112*, 1232–1268.

76. Stock, N., and Biswas, S. (2012). Synthesis of metal-organic frameworks (MOFs): routes to various MOF topologies, morphologies, and composites. Chem. Rev. *112*, 933–969.

77. Fu, G., Liu, W., Feng, S., and Yue, X. (2012). Prussian blue nanoparticles operate as a new

generation of photothermal ablation agents for cancer therapy. Chem. Commun. (Camb.) *48*, 11567–11569.

78. Cai, X., Gao, W., Zhang, L., Ma, M., Liu, T., Du, W., Zheng, Y., Chen, H., and Shi, J. (2016). Enabling prussian blue with tunable localized surface plasmon resonances: simultaneously enhanced dual-mode imaging and tumor photothermal therapy. ACS Nano *10*, 11115–11126.

79. Maaoui, H., Jijie, R., Pan, G.-H., Drider, D., Caly, D., Bouckaert, J., Dumitrascu, N., Chtourou, R., Szunerits, S., and Boukherroub, R. (2016). A 980nm driven photothermal ablation of virulent and antibiotic resistant Gram-positive and Gram-negative bacteria strains using Prussian blue nanoparticles. J. Colloid Interface Sci. *480*, 63–68.

80. Li, J., Liu, X., Tan, L., Cui, Z., Yang, X., Liang, Y., Li, Z., Zhu, S., Zheng, Y., Yeung, K.W.K., et al. (2019). Zinc-doped Prussian blue enhances photothermal clearance of *Staphylococcus aureus* and promotes tissue repair in infected wounds. Nat. Commun. *10*, 4490.

81. Liu, Z., Tan, L., Liu, X., Liang, Y., Zheng, Y., Yeung, K.W.K., Cui, Z., Zhu, S., Li, Z., and Wu, S. (2020). Zn^{2+}-assisted photothermal therapy for rapid bacteria-killing using biodegradable humic acid encapsulated MOFs. Colloids Surf. B Biointerfaces *188*, 110781.

82. Han, D., Li, Y., Liu, X., Li, B., Han, Y., Zheng, Y., Yeung, K.W.K., Li, C., Cui, Z., Liang, Y., et al. (2020). Rapid bacteria trapping and killing of metal-organic frameworks strengthened photo-responsive hydrogel for rapid tissue repair of bacterial infected wounds. Chem. Eng. J. *396*, 125194.

83. Lin, Y., Han, D., Li, Y., Tan, L., Liu, X., Cui, Z., Yang, X., Li, Z., Liang, Y., Zhu, S., et al. (2019). $Ag2_S$@WS_2 heterostructure for rapid bacteria-killing using near-infrared light. ACS Sustain. Chem. Eng. *7*, 14982–14990.

84. Gargioni, C., Borzenkov, M., D'Alfonso, L., Sperandeo, P., Polissi, A., Cucca, L., Dacarro, G., Grisoli, P., Pallavicini, P., D'Agostino, A., and Taglietti, A. (2020). Self-assembled monolayers of copper sulfide nanoparticles on glass as antibacterial coatings. Nanomaterials (Basel) *10*, 352.

85. Zhu, S., Gong, L., Xie, J., Gu, Z., and Zhao, Y. (2017). Design, synthesis, and surface modification of materials based on transition-metal dichalcogenides for biomedical applications. Small Methods *1*, 1700220.

86. Zhang, X., Zhang, G., Zhang, H., Liu, X., Shi, J., Shi, H., Yao, X., Chu, P.K., and Zhang, X. (2020). A bifunctional hydrogel incorporated with CuS@MoS_2 microspheres for disinfection and improved wound healing. Chem. Eng. J. *382*, 122849.

87. Jung, H.S., Verwilst, P., Sharma, A., Shin, J., Sessler, J.L., and Kim, J.S. (2018). Organic molecule-based photothermal agents: an expanding photothermal therapy universe. Chem. Soc. Rev. *47*, 2280–2297.

88. Kim, J.-W., Shashkov, E.V., Galanzha, E.I., Kotagiri, N., and Zharov, V.P. (2007). Photothermal antimicrobial nanotherapy and nanodiagnostics with self-assembling carbon nanotube clusters. Lasers Surg. Med. *39*, 622–634.

89. Li, Y., Liu, X., Tan, L., Cui, Z., Yang, X., Zheng, Y., Yeung, K.W.K., Chu, P.K., and Wu, S. (2018). Rapid sterilization and accelerated wound healing using Zn^{2+} and graphene oxide modified g-C_3N_4 under dual light irradiation. Adv. Funct. Mater. *28*, 1800299.

90. Xiang, Y., Mao, C., Liu, X., Cui, Z., Jing, D., Yang, X., Liang, Y., Li, Z., Zhu, S., Zheng, Y., et al. (2019). Rapid and superior bacteria killing of carbon quantum dots/ZnO decorated injectable folic acid-conjugated PDA hydrogel through dual-light triggered ROS and membrane permeability. Small *15*, e1900322.

91. Yu, Y., Mei, L., Shi, Y., Zhang, X., Cheng, K., Cao, F., Zhang, L., Xu, J., Li, X., and Xu, Z. (2020). Ag-conjugated graphene quantum dots with blue light-enhanced singlet oxygen generation for ternary-mode highly-efficient antimicrobial therapy. J. Mater. Chem. B Mater. Biol. Med. *8*, 1371–1382.

92. Xu, Y., Ma, J., Han, Y., Xu, H., Wang, Y., Qi, D., and Wang, W. (2020). A simple and universal strategy to deposit Ag/polypyrrole on various substrates for enhanced interfacial solar evaporation and antibacterial activity. Chem. Eng. J. *384*, 123379.

93. Zare, E.N., Makvandi, P., Ashtari, B., Rossi, F., Motahari, A., and Perale, G. (2020). Progress in conductive polyaniline-based nanocomposites for biomedical applications: a review. J. Med. Chem. *63*, 1–22.

94. Wong, T.W., Liao, S.Z., Ko, W.C., Wu, C.J., Wu, S.B., Chuang, Y.C., and Huang, I.H. (2019). Indocyanine green-mediated photodynamic therapy reduces methicillin-resistant *Staphylococcus aureus* drug resistance. J. Clin. Med. *8*, 411.

95. Wu, B., Fu, J., Zhou, Y., Wang, J., Feng, X., Zhao, Y., Zhou, G., Lu, C., Quan, G., Pan, X., and Wu, C. (2019). Metal-organic framework-based chemo-photothermal combinational system for precise, rapid, and efficient antibacterial therapeutics. Pharmaceutics *11*, 463.

96. Korupalli, C., Huang, C.C., Lin, W.C., Pan, W.Y., Lin, P.Y., Wan, W.L., Li, M.J., Chang, Y., and Sung, H.W. (2017). Acidity-triggered charge-convertible nanoparticles that can cause bacterium-specific aggregation in situ to enhance photothermal ablation of focal infection. Biomaterials *116*, 1–9.

97. Yan, L., Chen, L., Zhao, X., and Yan, X. (2020). PH switchable nanoplatform for *in vivo* persistent luminescence imaging and precise photothermal therapy of bacterial infection. Adv. Funct. Mater. *30*, 1909042.

98. Liu, H., Yang, Y., Liu, Y., Pan, J., Wang, J., Man, F., Zhang, W., and Liu, G. (2020). Melanin-like nanomaterials for advanced biomedical applications: a versatile platform with extraordinary promise. Adv. Sci. *7*, 1903129.

99. Ibelli, T., Templeton, S., and Levi-Polyachenko, N. (2018). Progress on utilizing hyperthermia for mitigating bacterial infections. Int. J. Hyperthermia *34*, 144–156.

100. Feng, Y., Liu, L., Zhang, J., Aslan, H., and Dong, M. (2017). Photoactive antimicrobial nanomaterials. J. Mater. Chem. B Mater. Biol. Med. *5*, 8631–8652.

101. Cheeseman, S., Christofferson, A.J., Kariuki, R., Cozzolino, D., Daeneke, T., Crawford, R.J., Truong, V.K., Chapman, J., and Elbourne, A. (2020). Antimicrobial metal nanomaterials: from passive to stimuli-activated applications. Adv. Sci. *7*, 1902913.

102. Yougbare, S., Chang, T.K., Tan, S.H., Kuo, J.C., Hsu, P.H., Su, C.Y., and Kuo, T.R. (2019). Antimicrobial gold nanoclusters: recent developments and future perspectives. Int. J. Mol. Sci. *20*, 2924.

103. Wang, C., Li, J., Liu, X., Cui, Z., Chen, D.F., Li, Z., Liang, Y., Zhu, S., and Wu, S. (2020). The rapid photoresponsive bacteria-killing of Cu-doped MoS_2. Biomater. Sci. *8*, 4216–4224.

104. Wang, X., Su, K., Tan, L., Liu, X., Cui, Z., Jing, D., Yang, X., Liang, Y., Li, Z., Zhu, S., et al. (2019). Rapid and highly effective noninvasive disinfection by hybrid Ag/CS@MnO_2 nanosheets using near-infrared light. ACS Appl. Mater. Interfaces *11*, 15014–15027.

105. Yang, T., Wang, D., and Liu, X. (2020). Antibacterial activity of an NIR-induced Zn ion release film. J. Mater. Chem. B Mater. Biol. Med. *8*, 406–415.

106. Huang, Y., Gao, Q., Li, X., Gao, Y., Han, H., Jin, Q., Yao, K., and Ji, J. (2020). Ofloxacin loaded MoS_2 nanoflakes for synergistic mild-temperature photothermal/antibiotic therapy with reduced drug resistance of bacteria. Nano Res. *13*, 2340–2350.

107. Ma, M., Liu, X., Tan, L., Cui, Z., Yang, X., Liang, Y., Li, Z., Zheng, Y., Yeung, K.W.K., and Wu, S. (2019). Enhancing the antibacterial efficacy of low-dose gentamicin with 5 minute assistance of photothermy at 50°C. Biomater. Sci. *7*, 1437–1447.

108. Wang, H., Song, Z., Li, S., Wu, Y., and Han, H. (2019). One stone with two birds: functional gold nanostar for targeted combination therapy of drug-resistant *Staphylococcus aureus* infection. ACS Appl. Mater. Interfaces *11*, 32659–32669.

109. Tan, L., Zhou, Z., Liu, X., Li, J., Zheng, Y., Cui, Z., Yang, X., Liang, Y., Li, Z., Feng, X., et al. (2020). Overcoming multidrug-resistant MRSA using conventional aminoglycoside antibiotics. Adv. Sci. *7*, 1902070.

110. Yang, Y., Deng, Y., Huang, J., Fan, X., Cheng, C., Nie, C., Ma, L., Zhao, W., and Zhao, C. (2019). Size-transformable metal-organic framework-derived nanocarbons for localized chemo-photothermal bacterial ablation and wound disinfection. Adv. Funct. Mater. *29*, 1900143.

111. Şen Karaman, D., Ercan, U.K., Bakay, E., Topaloğlu, N., and Rosenholm, J.M. (2020). Evolving technologies and strategies for combating antibacterial resistance in the advent of the postantibiotic era. Adv. Funct. Mater. *30*, 1908783.

112. Wang, Y., Yang, Y., Shi, Y., Song, H., and Yu, C. (2020). Antibiotic-free antibacterial strategies enabled by nanomaterials: progress and perspectives. Adv. Mater. *32*, e1904106.

113. Budimir, M., Jijie, R., Ye, R., Barras, A., Melinte, S., Silhanek, A., Markovic, Z.,

Szunerits, S., and Boukherroub, R. (2019). Efficient capture and photothermal ablation of planktonic bacteria and biofilms using reduced graphene oxide-polyethyleneimine flexible nanoheaters. J. Mater. Chem. B Mater. Biol. Med. *7*, 2771–2781.

114. Gao, G., Jiang, Y.W., Jia, H.R., and Wu, F.G. (2019). Near-infrared light-controllable on-demand antibiotics release using thermo-sensitive hydrogel-based drug reservoir for combating bacterial infection. Biomaterials *188*, 83–95.

115. Mei, L., Lin, C., Cao, F., Yang, D., Jia, X., Hu, S., Miao, X., and Wu, P. (2019). Amino-functionalized graphene oxide for the capture and photothermal inhibition of bacteria. ACS Appl. Nano Mater. *2*, 2902–2908.

116. He, D., Yang, T., Qian, W., Qi, C., Mao, L., Yu, X., Zhu, H., Luo, G., and Deng, J. (2018). Combined photothermal and antibiotic therapy for bacterial infection via acidity-sensitive nanocarriers with enhanced antimicrobial performance. Appl. Mater. Today *12*, 415–429.

117. Wang, W., Li, B., Yang, H., Lin, Z., Chen, L., Li, Z., Ge, J., Zhang, T., Xia, H., and Li, L. (2020). Efficient elimination of multidrug-resistant bacteria using copper sulfide nanozymes anchored to graphene oxide nanosheets. Nano Res. *13*, 2156–2164.

118. Zou, X., Zhang, L., Wang, Z., and Luo, Y. (2016). Mechanisms of the antimicrobial activities of graphene materials. J. Am. Chem. Soc. *138*, 2064–2077.

119. Qiu, J., Wang, D., Geng, H., Guo, J., Qian, S., and Liu, X. (2017). How oxygen-containing groups on graphene influence the antibacterial behaviors. Adv. Mater. Interfaces *4*, 1700228.

120. Fan, X., Yang, F., Huang, J., Yang, Y., Nie, C., Zhao, W., Ma, L., Cheng, C., Zhao, C., and Haag, R. (2019). Metal-organic-framework-derived 2D carbon nanosheets for localized multiple bacterial eradication and augmented anti-infective therapy. Nano Lett. *19*, 5885–5896.

121. Nima, Z.A., Watanabe, F., Jamshidi-Parsian, A., Sarimollaoglu, M., Nedosekin, D.A., Han, M., Watts, J.A., Biris, A.S., Zharov, V.P., and Galanzha, E.I. (2019). Bioinspired magnetic nanoparticles as multimodal photoacoustic, photothermal and photomechanical contrast agents. Sci. Rep. *9*, 887.

122. Moorcroft, S.C.T., Jayne, D.G., Evans, S.D., and Ong, Z.Y. (2018). Stimuli-responsive release of antimicrobials using hybrid inorganic nanoparticle-associated drug-delivery systems. Macromol. Biosci. *18*, e1800207.

123. Jiang, T., Wang, Y., Li, Z., Aslan, H., Sun, L., Sun, Y., Wang, W., and Yu, M. (2019). Prussian blue-encapsulated Fe_3O_4 nanoparticles for reusable photothermal sterilization of water. J. Colloid Interface Sci. *540*, 354–361.

124. Yu, S., Li, G., Liu, R., Ma, D., and Xue, W. (2018). Dendritic Fe_3O_4@poly(dopamine) @PAMAM nanocomposite as controllable NO-releasing material: a synergistic photothermal and NO antibacterial study. Adv. Funct. Mater. *28*, 1707440.

125. Mao, C., Xiang, Y., Liu, X., Zheng, Y., Yeung, K.W.K., Cui, Z., Yang, X., Li, Z., Liang, Y., Zhu, S., and Wu, S. (2019). Local photothermal/photodynamic synergistic therapy by disrupting bacterial membrane to accelerate reactive oxygen species permeation and protein leakage. ACS Appl. Mater. Interfaces *11*, 17902–17914.

126. Han, D., Han, Y., Li, J., Liu, X., Yeung, K.W.K., Zheng, Y., Cui, Z., Yang, X., Liang, Y., Li, Z., et al. (2020). Enhanced photocatalytic activity and photothermal effects of cu-doped metal-organic frameworks for rapid treatment of bacteria-infected wounds. Appl. Catal. B *261*, 118248.

127. Huang, B., Tan, L., Liu, X., Li, J., and Wu, S. (2018). A facile fabrication of novel stuff with antibacterial property and osteogenic promotion utilizing red phosphorus and near-infrared light. Bioact. Mater. *4*, 17–21.

128. Tan, L., Li, J., Liu, X., Cui, Z., Yang, X., Zhu, S., Li, Z., Yuan, X., Zheng, Y., Yeung, K.W.K., et al. (2018). Rapid biofilm eradication on bone implants using red phosphorus and near-infrared light. Adv. Mater. *30*, e1801808.

129. Luo, Y., Li, J., Liu, X., Tan, L., Cui, Z., Feng, X., Yang, X., Liang, Y., Li, Z., Zhu, S., et al. (2019). Dual metal–organic framework heterointerface. ACS Cent. Sci. *5*, 1591–1601.

130. Zhang, J., Sun, Y., Zhao, Y., Liu, Y., Yao, X., Tang, B., and Hang, R. (2019). Antibacterial ability and cytocompatibility of Cu-incorporated Ni-Ti-O nanopores on NiTi alloy. Rare Metals *38*, 552–560.

131. Wei, T., Tang, Z., Yu, Q., and Chen, H. (2017). Smart antibacterial surfaces with switchable bacteria-killing and bacteria-releasing capabilities. ACS Appl. Mater. Interfaces *9*, 37511–37523.